Non-equilibrium time-dependent solution to discrete choice with social interactions

James Holehouse[1]*, **Hector Pollitt**[2]

1 School of Biological Sciences, University of Edinburgh, Edinburgh, United Kingdom, **2** The World Bank, Washington, DC, United States of America

* james.holehouse@ed.ac.uk

Abstract

We solve the binary decision model of Brock and Durlauf (2001) *in time* using a method reliant on the resolvent of the master operator of the stochastic process. Our solution is valid when not at equilibrium and can be used to exemplify path-dependent behaviours of the binary decision model. The solution is computationally fast and is indistinguishable from Monte Carlo simulation. Well-known metastable effects are observed in regions of the model's parameter space where agent rationality is above a critical value, and we calculate the time scale at which equilibrium is reached using a highly accurate method based on first passage time theory. In addition to considering selfish agents, who only care to maximise their own utility, we consider altruistic agents who make decisions on the basis of maximising global utility. Curiously, we find that although altruistic agents coalesce more strongly on a particular decision, thereby increasing their utility in the short-term, they are also more prone to being subject to non-optimal metastable regimes as compared to selfish agents. The method used for this solution can be easily extended to other binary decision models, including Kirman's model of ant recruitment Kirman (1993), and under reinterpretation also provides a time-dependent solution to the mean-field Ising model. Finally, we use our time-dependent solution to construct a likelihood function that can be used on non-equilibrium data for model calibration. This is a rare finding, since often calibration in economic agent based models must be done without an explicit likelihood function. From simulated data, we show that even with a well-defined likelihood function, model calibration is difficult unless one has access to data representative of the underlying model.

1 Introduction

It has been 20 years since the publication of *discrete choice with social interactions* [1], which at the time of writing has over two thousand citations. The success of the publication has spawned a multitude of related publications, all with an interest in modelling how *variably rational* economic agents make decisions under exogenous influence in a system with collective endogenous interactions. More explicitly, the model of Brock and Durlauf considers a system of agents where each agent makes a decision *left* or *right*, where their decision is influenced by global influences (affecting all agents) and collective effects relating to

conformity forces between the agents (the more agents deciding one way, the stronger the influence on agents deciding the other way to change their minds). This simple but enlightening model has been extended in various directions in recent years, to multiple choice scenarios [2], towards models integrating heterogeneous agents in complex networks in the *random field Ising model* (RFIM) [3], and studying hysteresis in economic networks [4]. The binary decision model has similarities to other situations beyond binary choice, a famous example being the mean-field analysis done by Kirman et al. in studies of the Marseille fish market in order to explain the dynamics of how partially-rational, partially-loyal agents choose sellers of fish [5–7]. The study of such models is partially motivated by their simplicity compared to more general models, but also since they seem to be able to replicate some real socio-economic phenomena even given their simplicity.

One of the extensions of the binary decision model is the generalised model of Bouchaud in [3]. Therein, he proposed the RFIM as a unifying framework for the study of socio-economic phenomena, which subscribes agents as being heterogeneous (being predisposed to one decision over another), in a complex network of (possibly non-symmetric) interactions, subject to a global zeitgeist which in principle can change in time. This model is incredibly rich and its dynamics in some cases are described by evolving metastable states and long waiting times to reach equilibrium, very similar to known phenomena from the study of *spin glasses* in physics [8]. However, the downsides of the RFIM lie not in its ability to represent near infinite different realisations, but instead that this complexity restricts the possibility of solving such models analytically. This additionally makes model calibration from such models extremely difficult since the models are often made up of tens of parameters describing the probability distributions for the connections between agents, agent heterogeneity and the time-dependence of the zeitgeist. Therefore, although the RFIM can likely provide realistic descriptions of real-world socio-economic phenomena, the binary decision model of Brock and Durlauf is likely to provide the ideal starting point for model calibration and analytics of real data. We note that Brock and Durlauf's model is very closely related to Kirman's model of ant rationality (which is also known as the Moran model [9]), with the difference being in the choice of the transition rates between the two possible decisions [7, 10–12].

One can in fact draw an analogy to the field of Systems Biology, which uses mathematical models to describe the expression of mRNA and proteins from genes in the DNA [13, 14]. In reality, genes interact with proteins produced by other genes (and even their own proteins), which can be visualised as a gene regulatory network made up of many different network patterns known as motifs [15]. However, for practical reasons, researchers often ignore the complex interactions present in gene regulatory networks and instead describe genes of interest using a more simplified description. This simplified mechanism is known as the *telegraph model*, and it considers each gene as an on/off switch (either it can produce mRNA or it cannot), a model made up of four rate parameters rather than the potentially hundreds that would be necessary to describe the regulatory network of a particular gene (see [16–18] describing the mathematics and utility of the telegraph model). Experimental gene expression data is then calibrated to these models to give the set of four parameters (for each gene) describing the simplified model (see [19–23] where experimental data is fit to telegraph models). In the case of binary decisions, although network effects are important for some situations, as Brock and Durlauf [24] and Kirman state [6]: *one should be careful not to overemphasise network effects unless one has an empirical reason to infer their importance.* Hence, in the same way that the telegraph model provides a simplified description of gene expression, the model of Brock and Durlauf [1] provides a simple go-to model with which to classify different binary decision situations via a small number of parameters.

However, for all the applause of the model of Brock and Durlauf, the solution that they provide for the binary choice model *applies only at equilibrium*, whereas it is now widely known that the time to reach equilibrium, for many socio-economic systems of interest, does not occur on an economically relevant time scale [3, 25]. Hence, to understand binary decision phenomena more deeply one must consider the whole time-evolution of the dynamics from an initial condition to the equilibrium. In particular, model calibration is likely to be greatly perturbed using a likelihood function based on the equilibrium solution for data trajectories that are not a sample of the equilibrium distribution. In this paper we solve for the probability distribution of the mean-field binary decision model of Brock and Durlauf *in time*, and use our solution to investigate metastability, and the requirements on economic data necessary for model calibration. The method used for our solution also solves Kirman's ant model for the case of discrete numbers of agents, complementary to the study of [11], where a time-dependent solution is provided for a continuous number of agents (i.e., the large agent population limit). This analytic solution allows for faster model calibration compared to simulation based approaches, as well as the analytical construction of a likelihood function.

The paper is structured as follows. In Section 2 we introduce the mean-field binary decision model of Brock and Durlauf starting from the RFIM of Bouchaud [3]. In this way the reader can see how the mean-field description comes from applying various assumptions to the RFIM. Section 2.1 describes the situation of a system of selfish agents who make decisions such that they maximise their utility (if they are rational). In Section 2.2 we extend this analysis to a system of altruistic agents, where now agents are concerned with optimising the global utility. Then in Section 2.3 we solve the mean-field binary decision model in time. Throughout Section 3 we explore the solution that we have found the metastable phenomena it possesses (known as a lock-in in the economics community). In the process, using a first passage time analysis, we outline a method to very accurately determine the time scales of these metastable states. In Section 4 we use our time-dependent solution to construct a likelihood function that can be used for model calibration, and assess the conditions necessary on simulated data to provide accurate calibration. We then compare the results from our model to the standard tenets of neoclassical economics in Section 5, before concluding our paper in Section 6.

2 Binary decision model

2.1 Selfish agents

Consider a system of N economic agents where each agent i can choose between two distinct decisions, *left* denoted by $S_i(t) = -1$, and *right* denoted by $S_i(t) = 1$. Left or right could correspond to an infinite number of binary choice questions, for example, to vote either Democrat or Republican, to buy one stock or another, or whether one is participating in the latest fashion trend (in this case yes or no). Depending on the question one is considering, the model parameters making up a binary decision model are likely to be very different. For example, a binary decision model of an American election is unlikely to have the same model parameters as one describing consumers choosing between two brands of similar cereal: in the case of a cereal, the exogenous influence of advertising is more important than endogenous effects, whereas the collective effects are likely more important in an election model. The attribute $S_i(t)$ denotes the decision currently made by agent i at a time t, with the state of the entire system at time t being given by the set of choices made by all agents at that time, denoted $\mathcal{S} = \{S_1, S_2, \ldots, S_N\}$. The RFIM introduced by Bouchaud in [3] takes into account three main factors, all of which contribute to the influence on agent i, $I_i(t)$, which are (using naming conventions inspired by [3]):

1. The *personal inclination* (or predisposition) of the agent to favour one decision over the other. The contribution to $I_i(t)$ from personal inclination is $f_i \in [-\infty, \infty]$, where $f_i < 0$ means a predisposition to left and $f_i > 0$ means a predisposition to right. In principle, these heterogeneities could be time-dependent, but since they are difficult to empirically quantify one generally assumes they are constant.

2. The *zeitgeist*, a global influence equally affecting all agents, such as news reporting or stock trends. Its contribution to $I_i(t)$ is given by $F(t) \in [-\infty, \infty]$, and we assume its time-dependence directly since it is often global effects (e.g., stock market decline or warming global temperature) that change in time.

3. *Agent-to-agent interactions*, attractive/repulsive influences for the agents to attract/repel others from their same view. The strengths of these interactions are stored in the matrix $\mathbf{J}$, where $J_{ij} \equiv [\mathbf{J}]_{ij}$ is the contribution of agent j to $I_i(t)$ such that the total contribution of all agents in neighbourhood v_i to the influence of agent i is $\sum_{j \in v_i} J_{ij} S_j(t)$.

In summary, each agent is subject to an *influence*, $I_i(t)$, which is the sum of these contributions,

$$I_i(\mathcal{S}, t) = f_i + F(t) + \sum_{j \in v_i} J_{ij} S_j(t). \tag{1}$$

The importance of the influence is that, where agents are rational, they will aspire to make a decision (left or right) that agrees with the influence they are subjected to. We explore the mechanisms through which agents update their decisions below, based on the introduction of an agent utility function.

In the mean-field case several simplifications can be made. The main assumption is that all agents are equally connected to each other with strength J meaning that each agent only responds to the average global opinion of all agents $m = \sum_i S_i / N$. As has been widely documented, *the mean-field approximation is qualitatively a good approximation for nearest neighbour interactions where $N \gg 1$ and the number of dimensions $d \geq 4$ or in situations where agents are connected to many other agents* [26]. We additionally rescale J by the number of agents $J \rightarrow J/N$, such that the agent-to-agent interaction contribution to $I_i(\mathcal{S}, t)$ is intensive. Finally, we assume that each agent has the same personal inclination f, a factor that is absorbed into the definition of the $F(t)$ in Eq (1). Note that even in the absence of personal preference the agents are still heterogeneous in the sense that they make their own decisions *at different times*. Within this set of approximations the information is a shared function amongst all agents and is given by,

$$I_i(\mathcal{S}, t) \equiv I(n(t), t) = F(t) + Jm(n(t)), \tag{2}$$

where we reinterpret the definition of $m(n(t)) = (2n(t) - N)/N$, where $n(t)$ is the number of agents whose decision at t is right (with $N - n(t)$ deciding left). For brevity, we will often drop the time-dependence of n on t, although it is always implicit. The function $m(n)$, as well as being the average global opinion, is the *order parameter* of the system and takes discrete values in $[-1, 1]$ for finite N: $m(N) = 1$ if all agents take the right decision, $m(N/2) = 0$ if equal numbers decide right and left, and $m(0) = -1$ if all agents decide left. Hence, $m(n)$ appropriately characterises the state of the system for any value of N.

In the mean-field context one can interpret the meanings of $F(t)$, J and $m(n)$ in many ways. One way, introduced in [3], is to interpret $F(t)$ as the cost of installing a new heating system and $Jm(n(t))$ as the expected cost decrease as technical improvements cause more people to switch to the dominant technology. A similar interpretation will be used later on in Section 3.1

to discuss the phenomena of technology lock-ins. In many settings, mean-field approximations are reasonable for binary choice decisions: many decisions one makes on a day-to-day basis are influenced by many peers acting around an individual, for example, deciding whether to invest in cryptocurrency [27], or the language one uses in online reviews [28]. As noted by Kirman [6], *sociologists have long observed empirically that relational networks are likely to be much more connected than one might imagine*. However, in many cases network effects are very relevant, for example, children brought up in religious households are much more likely to be religious themselves [29], in which case the mean-field assumption is a poor one. We illustrate the concept of the mean-field assumption in Fig 1(a).

We now introduce the utility of agent i as $U_i(n, t) \equiv S_i(t)I_i(\mathcal{S}, t) = S_i(t)I(n, t)$, a quantity that a rational agent would want to maximise over any realisation of the model. We denote the situation wherein agents only care to maximise their own utility as a system of *selfish agents* and generalise for more altruistic agents that are motivated by changes in the global utility in the following section. Now consider that the rate at which an agent changes their mind is
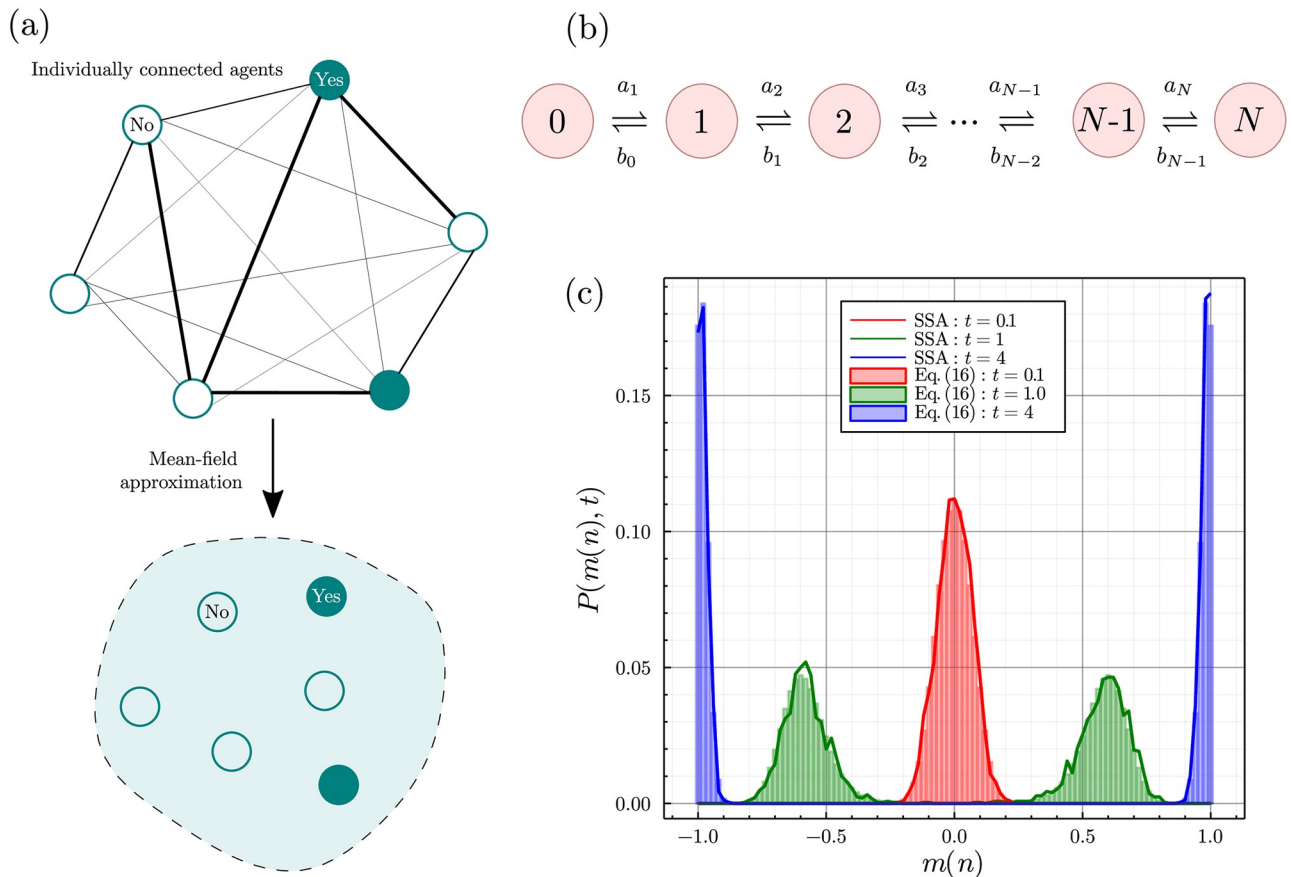
Fig 1. (a) Illustration showing the effect of mean-field theory on a network of interconnected agents that influence each others decisions. In the mean-field case each agent is influenced by the same information $I(n, t)$ which they all contribute towards. (b) Diagram showing the 1D process that is equivalent to the mean-field case of the binary decision model. The number in each circle denotes the number of *right deciding* agents, and the expressions above and below the arrows denote the associated probabilities of transitioning between each configuration. (c) Plots showing the correspondence between our analytic solution in Eq (16) and Monte Carlo simulations provided by the SSA. The parameters for this time-evolution are $F = 0$, $J = 10$, $\alpha = 0$, $\beta = 1$, $\gamma = 1$, $N = 100$ and $P(n, 0) = \delta_{n,N/2}$. The probability distribution from the SSA is calculated from 2.5×10^3 trajectories. As $t \to \infty$ we see the emergence of a single steady-state consisting of two equal modes of height ≈ 0.5 at $m(0) = -1$ and $m(N) = 1$. In the limit $N \to \infty$ this steady-state bimodality corresponds to symmetry breaking behaviour [30]. Note that the SSA simulations in the solid lines show random perturbations due to the stochastic nature of the simulations, whereas the bars showing Eq (16) do not show these deviations.

dependent on *the change in their own utility if they do change their mind*. For agent i, whose utility at time t is $U(n, t)$, changing their decision from $S_i \rightarrow -S_i$ at time t would result in the utility change,

$$\Delta U_i(n, t) \equiv U_i(n - S_i, t) - U_i(n, t) = -2S_i(t)I(n, t) + 2J/N. \qquad (3)$$

Note that $2J/N$ is a self-interaction term which comes from considering the change in $m(n)$ as $S_i \rightarrow -S_i$, a contribution that equally affects the rates of transition from $-1 \rightarrow 1$ and $1 \rightarrow -1$, and that is negligible for $N \gg 1$. In the case where the change in the agent's decision is not assumed to affect $\Delta U_i(n, t)$ the term $2J/N$ can be ignored. If an agent had made decision $S_i(t) = -1$ (or $S_i(t) = 1$) and the influence on them was $I(n, t) > 0$ (or $I(n, t) < 0$) then in changing their decision at t they increase their utility; alternatively, if an agent had made decision $S_i(t) = -1$ (or $S_i(t) = 1$) and the influence on them was $I(n, t) < 0$ (or $I(n, t) > 0$) then in changing their decision at t they decrease their utility. Hence, a rational agent will (on average) make decisions such that their choice $S_i(t)$ agrees with the sign $I(n, t)$, at a rate (determined below) that is a monotonically increasing function of $\Delta U_i(n, t)$. *More simply, the larger the change in the agent's utility $\Delta U_i(n, t)$ upon a decision change, the larger the rate at which an agent changes their decision.*

In this paper we choose decision rules based on detailed balance considerations [30]. This means that we choose the rates with which agents update their decisions based on the assumption that as $t \rightarrow \infty$ the Boltzmann equilibrium distribution will be attained, i.e., $P_{eq}(S_i) \propto \exp(\beta U_i(n))$ where β is the rationality of agent i (discussed below). Enforcing detailed balance means the transition rates must satisfy,

$$\frac{W_n(S_i(t) \rightarrow -S_i(t))}{W_{n-S_i}(-S_i(t) \rightarrow S_i(t))} = \frac{\exp(\beta U_i(n - S_i, t))}{\exp(\beta U_i(n, t))} = \exp(\beta \Delta U_i(n, t)), \qquad (4)$$

where $W_n(S_i(t) \rightarrow -S_i(t))$ is the transition rate for agent i to change their decision from $S_i \rightarrow -S_i$ at time t given there are already n agents deciding *right* [30]. That $W_n(S_i(t) \rightarrow -S_i(t))$ is a transition rate means that in a time interval $[t, t + \Delta t)$ an agent will change their decision with probability $W_n(S_i(t) \rightarrow -S_i(t))\Delta t$. There are several conventional ways to prescribe the transition rates from Eq (4). A common way is to choose the Arrhenius form [31] where the transition probabilities become $W_n(S_i(t) \rightarrow -S_i(t)) = \gamma \exp(\beta U_i(n - S_i, t))$ and $W_{n-S_i}(-S_i(t) \rightarrow S_i(t)) = \gamma \exp(\beta U_i(n, t))$, where γ is a time scale parameter. An alternate form, and the form we use in this paper, are the Glauber/logit transition rates, which are given by [3, 32, 33]:

$$W_n(S_i(t) \rightarrow -S_i(t)) = \frac{\gamma}{1 + \exp(-\beta \Delta U_i(n, t))} \qquad (5)$$

The choice of logit transition rates is motivated by [33], which derives Eq (5) using the maximum entropy principle. This assumes that agents make their choices based on a compromise between short-term utility gain and a desire to sample other available choices. We note that the Arrhenius transition rates do not subscribe to this interpretation, since as is clear from their form, the transition rates are only dependent on the utility of the agent upon the change in decision; i.e., the agents do not consider the change in decision based on a knowledge of all decisions they could take, only the one they will take. In reality the proper form of the transition rates likely varies depending on the problem at hand. However, it seems likely that in the case of a binary decision an agent would need to first explore a range of decisions before they know the one that maximises their utility, hence we use Eq (5) for the rest of the paper. In other models the logit-like behaviour arises from other considerations, for example their

presence in the *future technology transformation* (FTT) models described in [34] is attributed to probabilistic nature of the cost of two competing technologies (see Fig 1 of [35]). One also observes that the dependence of the propensity function W_n on the change in utility is identical to that seen in classical choice theory [36]; this is by design, and the propensity of an agent to change their decision is proportional to the probability that the agent would indeed choose that option in choice theory.

Eq (5) allows us to explore the agent rationality β, which is a direct analogue of the inverse temperature commonly seen in equilibrium thermodynamics and statistical physics [30]. As $\beta \to 0$ the agents become completely irrational and changes of decision occur at the same rate $\gamma/2$ regardless of an agent's utility change. Conversely, as $\beta \to \infty$ each agent is completely rational and Eq (5) becomes,

$$\lim_{\beta \to \infty} W_n(S_i(t) \to -S_i(t)) = \begin{cases} 0, & \Delta U_i(t) < 0, \\ \gamma, & \Delta U_i(t) > 0. \end{cases}$$

Hence, completely rational agents *always* make decisions that agree with the influence upon them. For intermediate values of β we obtain the typical 'S-shaped' adoption curves with respect to $\Delta U_i(t)$, a common feature of many macroeconomic models including heterogeneous agents [34, 37, 38]. We note that since β is a constant we are implicitly assuming that each agent has the same level of rationality. Although in reality it may not be the case, for most situations we assume it to be a good approximation.

In the model described above 'completely rational' agents correspond to agents that on their next change of decision, only choose the option that maximises their utility. So in a sense, even completely rational agents have limited foresight since they make decisions only based on the current state of the system, and not based on which decision in the long-run will optimise their utility—which would be the decision agreeing with the sign of F. Clearly, even these hyper-rational agents do not agree with the 'perfect rationality' of agents observed in neoclassical economics (where agents even optimise for future conditions [39]). The agents in the binary decision model more closely correspond to Keynesian agents with 'fundamental uncertainty' in economies driven by short-term optimism (in our case short-term utility gain) [40].

In contrast to the above, Kirman's model of ant rationality [10] assumes a different form of propensities than the logit form seen in Eq (5). Interpreting $S_i(t) = \pm 1$ now as two different sources of food and n as the number of ants at the right-hand (+1) food source, ants switch food source due to two influences: the first is due to random switching with probability ϵ per unit time, the second due to recruitment by another ant with probability μ per unit time. The former is akin to an effective reaction with first-order kinetics, whereas the latter is akin to a reaction with second-order kinetics—i.e., the chance meeting of two ants is modelled as the probability of two molecules of the same species colliding. Following the laws of mass-action kinetics [14, 31, 41], the propensities for Kirman's ant model are then proportional to $W_n(-1 \to +1) = (N - n)\epsilon + \frac{\mu(N-n)n}{N-1}$ and $W_n(+1 \to -1) = n\epsilon + \frac{\mu(N-n)n}{N-1}$, as seen in [11]. We will see below in Section 2.3 that our method for solving the model of Brock and Durlauf in time also easily extends to Kirman's model, although we focus on the former model for the rest of the paper.

2.2 Altruistic agents

We now generalise our mean-field model of economic agents such that they can take into account changes in the *global utility* of all agents. We refer to this as *agent altruism* since in this case agents do not only think about maximising their own utility but that of the entire

population [42]. In the context of binary decisions, having agents with altruistic attributes is somewhat realistic. Take the example we made above relating $F(t)$ to the cost of a heating system and $Jm(n)$ as the reduction in cost given more agents are using the technology. In this example altruistic agents could further benefit the utility of all individuals by more quickly arriving at a state where all agents are in agreement with one another. We define the global utility simply as the sum of the utilities of all agents,

$$A(n, t) = \sum_{i=1}^{N} U_i(n, t). \tag{6}$$

Due to the mean-field interactions between the agents, a change in decision in one of the agents will change the utility of the individual agent by a different amount than the global utility. For example, say we have $\mathcal{S}_1 = \{S_1, \ldots, S_j, \ldots, S_N\}$ and at time t the system evolves to $\mathcal{S}_2 = \{S_1, \ldots, -S_j, \ldots, S_N\}$: in general we find that $A(n - S_j, t) - A(n, t) \neq U_j(n - S_j, t) - U_j(n, t)$, unless there are no interactions between the agents. We consider $A(n - S_i, t) - A(n, t)$ explicitly below.

Now consider a system of entirely altruistic agents, whose decisions do not depend on their individual utilities but only on $A(t)$. As we did before for the selfish agents, we want to calculate the change in the $A(t)$ if agent i changes their decision from $S_i \rightarrow -S_i$, i.e., $\Delta A_i(n, t) \equiv A_i(n - S_i, t) - A_i(n, t)$. Using Eq (6), one finds that this is given by,

$$\Delta A_i(n, t) = \Delta U_i(n, t) - 2JS_i\left(m(n) - \frac{S_i}{N}\right). \tag{7}$$

Hence, the change of the global utility is equal to the change in the individual utility of the agent minus a non-negligible term that accounts for the change in the utility of the rest of the population given agent i has changed their decision. Note that the $m(n) - S_i/N$ term comes from considering the sum over all agents aside from agent i, $\sum_{j \neq i} S_j = Nm(n) - S_i$, where the S_i/N term is negligible for $N \gg 1$. The extra term in Eq (7) has an intuitive meaning, whose presence is explained by two mechanisms: (i) if S_i (the original choice made by the agent) has the *same* sign as $m(n)$ then $\Delta A_i < \Delta U_i$ since the agent has decided to go against the average opinion of all other agents encoded in $m(n)$; (ii) if S_i has the *opposite* sign to $m(n)$ then $\Delta A_i > \Delta U_i$ since the agent has decided to go with the average opinion, having previously been against it.

Following previous work [42] we now introduce the *gain*, which gives a generalised form of utility change for agents that can be either entirely selfish, altruistic, or else somewhere in between. The gain for agent i in changing their decision from $S_i \rightarrow -S_i$ is defined by,

$$\begin{aligned} \mathcal{G}_i(n, t) \quad &\equiv \Delta U_i(n, t) + \alpha(\Delta A_i(n, t) - \Delta U_i(n, t)) \\ &= -2S_i(F(t) + Jm(n)(1 + \alpha)) + \frac{2(1 + \alpha)J}{N}, \end{aligned} \tag{8}$$

where α is a parameter such that $\alpha = 0$ corresponds to a system of selfish agents, $\alpha = 1$ a system of altruistic agents, and $0 < \alpha < 1$ somewhere in between. We can finally write our most general transition rates including the effects of agent altruism,

$$W_n(S_i(t) \rightarrow -S_i(t)) = \frac{\gamma}{1 + \exp(-\beta \mathcal{G}_i(n, t))}, \tag{9}$$

which is essentially identical to the decision rule of Eq. (1) in [42]. Curiously, and possibly somewhat intuitively, including the effects of altruism in our mean-field description acts to scale the agent-to-agent interaction strength by $1 + \alpha$. As we explore in Section 3, this scaling

of the endogenous strength can have qualitative as well as quantitative effects on the model. It seems the mean-field approximation is responsible for the simplicity of this scaling, since in the general case of the model introduced in Section 2 the difference in utility change between altruistic agents and selfish ones is found to be the less simplistic and given by $\Delta A_i - \Delta U_i = -2 \sum_{j \neq i} J_{ji} S_i S_j$. Note that for the case of generalised mean-field altruistic agents one can define a *Hamiltonian* $\mathcal{H}(\mathcal{S})$, a function of the state of the system $\mathcal{S}$ such that,

$$\Delta \mathcal{H}_i(\mathcal{S}, t) \equiv \mathcal{H}(\{S_1, \ldots, -S_i, \ldots, S_N\}, t) - \mathcal{H}(\{S_1, \ldots, S_i, \ldots, S_N\}, t) = \mathcal{G}_i(n, t). \quad (10)$$

One finds this function is given by,

$$\mathcal{H}(\mathcal{S}, t) = N m(n) \left(F(t) + \frac{1}{2}(\alpha + 1) J m(n) \right), \quad (11)$$

where we remind the reader that $m(n) = (2n - N)/N = \sum_i S_i / N$. The existence of $\mathcal{H}(\mathcal{S})$ ensures that decision rules based on Eq (9) satisfy detailed balance and that as $t \to \infty$ the equilibrium probability of each state is $P_{eq}(\mathcal{S}) \propto \exp(\beta \mathcal{H}(\mathcal{S}))$ for all $0 \leq \alpha \leq 1$.

2.3 Master equation and analytical time-dependent solution

We can now proceed to solve the mean-field model analytically. First we map the model to a stochastic birth-death reaction scheme given by,

$$L \underset{nl(n)}{\overset{(N-n)r(n)}{\rightleftharpoons}} R, \quad (12)$$

where $r(n)$ and $l(n)$ are the transition rates at which each agent changes their decision from *left to right* and *right to left* respectively given there are n right voting agents, and L and R are symbols representing agents who have decided left and right respectively. In this context one can state that a decision change of an agent is akin to a gain/loss of particles, where each particle denotes a right deciding agent [31]. *Importantly, from this birth-death mapping, where $F(t) \to F$ is a time-independent constant, it is clear that in the mean-field limit the number of right deciding agents n completely determines the state of the system.* Hence, for the moment we set $F(t) \to F$, and discuss the case of time-dependent $F(t)$ later on. The rates $r(n)$ and $l(n)$ are defined by the decision rules we derived above in Eq (9) and are explicitly given by,

$$\begin{aligned} r(n) &= W_n(-1 \to 1), \\ l(n) &= W_n(1 \to -1). \end{aligned} \quad (13)$$

Note that the choice of the overall propensities $(N - n)r(n)$ and $nl(n)$ comes from mass-action kinetics: in short, the rate of gaining a new right deciding agent is proportional to the number $N - n$ of left deciding agents in the system [14, 31].

One can easily check that by writing the rate equation for the evolution of Eq (12), in the large N limit, as $t \to \infty$ one recovers the classic mean-field result of $m = \tanh(\beta(F + J(\alpha + 1)m))$. However, we can do better than the rate equation describing the steady-state value of m, and can in fact solve for the probability of having n right deciding agents at a time t, $\mathcal{P}(n, t)$. We first write the master equation corresponding to the process in (12),

$$\partial_t \mathcal{P}(n, t) = [(N - (n-1))r(n-1)]\mathcal{P}(n-1, t) \quad + [(n+1)l(n+1)]\mathcal{P}(n+1, t) \\ - [(N-n)r(n) + nl(n)]\mathcal{P}(n, t). \quad (14)$$

The master equation, otherwise known as the Kolmogorov forward equation, is a set of first-order differential equations describing the time evolution of being in discrete state n at time t.

Eq (14) is a 1D master equation since it describing the evolution of only a single stochastic variable n. We outline the derivation of a 1D master equation from first principles in Sec. 1 in S1 File. At steady-state, where $\partial_t \mathcal{P}(n, t \to \infty) = 0$, 1D master equations are very well understood, and their properties are discussed in many textbooks [30, 31, 43]. Solving them in time is a much trickier problem. However, it is possible to solve Eq (14) and we do so using the non-standard and useful method of [44]. For readers that are less mathematically inclined we suggest that not too much time is spent on the derivation below; *it is simply most important to realise that the mean-field binary decision model can be solved in time, and that its analytical solution is much quicker to compute than simulation based methods*. For consistency with [44] publication we introduce the following notation: $a_n = (N - (n-1))r(n-1)$ and $b_n = (n+1)l(n+1)$, and we show the transitions between the microstates of the model using these propensities in Fig 1(b). Then, Eq (14) can be re-written as $\partial_t \vec{\mathcal{P}}(t) = \mathbf{A} \cdot \vec{\mathcal{P}}$, where $\vec{\mathcal{P}}(t)$ is the column vector $(\mathcal{P}(0, t), \mathcal{P}(1, t), \ldots, \mathcal{P}(N, t))$ and $\mathbf{A}$ is the *master operator*, a $(N+1) \times (N+1)$ tridiagonal matrix, given by,

$$\mathbf{A} = \begin{pmatrix} -a_1 & b_0 & & & \\ a_1 & -(b_0 + a_2) & b_1 & & \\ & a_2 & -(b_1 + a_3) & \ddots & \\ & & & \ddots & \ddots \end{pmatrix}. \tag{15}$$

We denote the eigenvalues of the matrix $\mathbf{A}$ as λ_i for $i = 1, 2, \ldots, N+1$, and from Perron-Frobenius theorem can state that the largest eigenvalue is $\lambda_1 = 0$ with $\lambda_1 > \text{Re}(\lambda_2) \geq \ldots \geq \text{Re}(\lambda_{N+1})$ [45]. Note that the eigenvector corresponding to $\lambda_1 = 0$ is the steady-state probability distribution. Following some complex analysis on the resolvent of the master operator and judicious use of Cauchy's residue theorem in [44] one then arrives at the solution of Eq (14) from an initial condition $\mathcal{P}(n, 0) = \delta_{n, n_0}$, explicitly,

$$P(m(n), t | m(n_0), 0) = \mathcal{P}(n, t | n_0, 0) = \begin{cases} b_n \cdots b_{n_0 - 1} \sum_{i=1}^{N+1} e^{\lambda_i t} \dfrac{p_n(\lambda_i) q_{n_0 + 2}(\lambda_i)}{\prod_{j \neq i}(\lambda_i - \lambda_j)}, & n < n_0, \\[4mm] \sum_{i=1}^{N+1} e^{\lambda_i t} \dfrac{p_n(\lambda_i) q_{n_0 + 2}(\lambda_i)}{\prod_{j \neq i}(\lambda_i - \lambda_j)}, & n = n_0, \\[4mm] a_{n_0 + 1} \cdots a_n \sum_{i=1}^{N+1} e^{\lambda_i t} \dfrac{p_{n_0}(\lambda_i) q_{n + 2}(\lambda_i)}{\prod_{j \neq i}(\lambda_i - \lambda_j)}, & n > n_0, \end{cases} \tag{16}$$

where the orthogonal polynomials p_n and q_n are recursively defined via,

$$p_1(y) = 1, \ p_2(y) = y + a_1, \tag{17}$$

$$p_i(y) = (y + a_i + b_{i-2}) p_{i-1}(y) - b_{i-2} a_{i-1} p_{i-2}(y), \tag{18}$$

$$q_{N+2}(y) = 1, \ q_{N+1} = y + b_{N-1}, \tag{19}$$

$$q_i(y) = (y + a_i + b_{i-2}) q_{i+1}(y) - b_{i-1} a_i q_{i+2}(y). \tag{20}$$

Eqs (16)–(20) constitute the analytical time-dependent solution for the mean-field Ising-

Weidlich binary decision model with variably selfish-altruistic agents [46]. Note that unlike $\mathcal{P}(n, t|n_0, 0)$, $P(m(n), t|m(n_0), 0)$ is not a probability density but instead the raw probability of the system having a certain value of $m(n)$ at time t, i.e., $\sum_n P(m(n)) = 1$ and $\sum_n P(m(n))\Delta m \neq 1$ (where $\Delta m = 1/N$). For details regarding the derivation of this result we refer the reader to [44]. In the most general case of usage of the model one needs to determine the eigenvalues of $\mathbf{A}$ computationally, which we do using the `eigvals` function in the Julia package `LinearAlgebra` [47]. However, since the eigenvectors are already implicit in the form of Eq (16) we do not need to evaluate these computationally, and hence the analytical solution we utilise can be computed much more quickly than a finite state projection approach requiring matrix exponentiation [48]. Note that the `eigvals` function that we use to compute the eigenvalues does not always return entirely real eigenvalues in every case (as one would physically expect) and often eigenvalues come in the form of a complex conjugate pairs. This is a common computational error, since we know theoretically that the eigenvalues should be real, and the resultant set of eigenvalues we obtain from `eigvals` is known as a *pseudospectrum* [49], which arises since the eigenvalues of these matrices are very sensitive to small perturbations.

Importantly however, the *usage of the pseudospectrum in* Eqs (16)–(20) *returns a normalised probability distribution that is indistinguishable from Monte Carlo simulation of the model*. The Monte Carlo simulation method we employ is known as the *stochastic simulation algorithm* (SSA), and we detail it in Sec. 3 in S1 File. Briefly, the SSA is a continuous time method often used in stochastic chemical kinetics to simulate chemical reactions. In our case, it outputs individual realisations of the master Eq (14), which can then be replicated as an ensemble in order to construct the probability distribution, mean and variance of the process in time. In Fig 1(c) we show that our analytic time-dependent solution corresponds precisely to the distribution produced via the SSA for times near the initial condition through to near steady-state conditions. In Section 3.2 we approximately calculate λ_2, the eigenvalue that determines the relaxation rate to the steady-state, using exact expressions for the switching times between lock-in states. Note that λ_2^{-1} gives the time scale to reach the equilibrium. We further note that an analytical procedure to calculate the eigenvalues of our problem in a perturbative sense may be possible following methods used in [50].

Eqs (16)–(20) assume that the initial condition is a fixed value of n_0 right deciding agents at $t = 0$. However, often the initial state is not precisely known but is itself a distribution $\mathcal{Q}(n) \equiv \mathcal{P}(n, 0)$. Using the laws of probability one determines the time evolution of $\mathcal{P}(n, t)$ with initial condition $\mathcal{Q}(n)$ as,

$$P(m(n), t|\mathbb{Q}(m(n)), 0) = \mathcal{P}(n, t|\mathcal{Q}(n), 0) = \sum_{n_0=0}^{N} \mathcal{Q}(n_0)\mathcal{P}(m(n), t|m(n_0), 0), \qquad (21)$$

where $\mathbb{Q}(m(n)) = \mathcal{Q}(n)$. In the common case where each agent is initially assigned a decision at random with probability p_0 the number of initially right deciding agents is drawn from a binomial distribution, i.e., $\mathcal{Q}(n) = \mathrm{Bin}(n; N, p_0)$. The steady-state distribution reached as $t \rightarrow \infty$, i.e., $\mathcal{P}_s(n) = \mathcal{P}(n, t \rightarrow \infty)$, is widely known for birth-death processes with general rates and can be expressed as the following from Kirchhoff's theorem [51],

$$P_s(m(n)) = \mathcal{P}_s(n) = \frac{(\prod_{i=1}^{n} a_i)(\prod_{i=n}^{N-1} b_i)}{\sum_j (\prod_{i=1}^{j} a_i)(\prod_{i=j}^{N-1} b_i)}, \qquad (22)$$

where we define the empty product $\prod_{j>i}^{i}$ as being equal to 1. $P_s(n)$ is independent of the initial condition, even for systems with long-time metastability/lock-in effects. Note that for the case of time-dependent $F(t)$ the solution above must be somewhat modified since a_i and b_i are no

longer dependent only on n but also explicitly on t. This case of having a zeitgeist that changes in time has important policy implications, and although it is not relevant for our work here we outline its solution in Sec. 3 in S1 File.

Finally, we note that if one interprets the economic agents as magnetic spins, the zeitgeist instead as a magnetic field, and J as the mean-field exchange coupling (multiplied by the number of nearest neighbours), then our time-dependent solution above also provides the solution to the mean-field Ising model for a finite number of N magnetic spins. This model of a magnet, famed for its simple equilibrium solution among other things, is still the subject of recent work [52–54].

3 Exploration of the model

We can now use our analytic time-dependent solution to explore the model in different regimes of parameter space. Before delving into metastable behaviours, which will occupy us for the rest of this section, we detail two well known features of the model [1, 3, 30]. The first is that, for $F = 0$, the model exhibits a phase transition at a critical value of agent rationality $\beta_c = 1/J(1 + \alpha)$. The origin of this critical value is explored in Sec. 4 in S1 File, but essentially for $\beta > \beta_c$ one finds a symmetry breaking behaviour wherein agents either mostly become left or right deciding at steady-state and $P_s(n)$ is bimodal; whereas for $\beta \leq \beta_c$ the steady-state distribution $P_s(n)$ is monomodal with a peak at $m = 0$. At $\beta = \beta_c$ we see the characteristic shape of a flat-topped steady-state distribution centred at $m = 0$ such that any small deviation above β_c causes bimodality. Secondly, for $F \neq 0$ one finds that although there may still exist two equilibrium modes of behaviour deterministically, in reality the decision of same sign to F is exponentially more favourable as $t \to \infty$ (shown explicitly in Section 3.2). Economically, what this means is that agents coalesce on the same decision when they are sufficiently rational and when collective effects are deemed at least as important as exogenous effects. A recent review of path-dependency effects similar to lock-ins is given in [55].

3.1 Lock-ins

Let's explore a possible narrative of the model and suppose the two decisions left and right correspond to two competing technologies. F accounts for any exogenous effects on the agents, for example, the cost difference between the two technologies or the effects of changing social norms. Denoting C_L and C_R as the weight of these real and social costs of the left and right technologies, one can the break down F into its constituent parts, i.e., $F = C_L - C_R$. On the other hand, the interaction term J takes into account any endogenous changes arising from within the dynamics of the model, in particular: (1) learning effects as technology gets improved due to increased uptake [56], (2) any endogenous changes in price due to the increased uptake [56, 57], and (3) establishment effects, accounting for the ease of investment regardless of the price since the infrastructure needed for the technology is already there [56]; i.e., $J = J_1 + J_2 + J_3$.

Importantly, the foresight of the agents is limited only to how their decision change at the current time changes their own (or global) utility, and they do not know *a priori* which technology is the optimal one (i.e., they cannot distinguish between exogenous and endogenous influences). The state of maximal utility for the agents will clearly be that where all agents decide on the optimal technology (leading to the highest utility amongst all agents), which has the best combined trade-off between price and social appropriateness. However, it has been observed that this does not always happen, and path-dependency can lead to people making collective decisions that differ from the optimal one. This leads to so called *lock-in* effects [58], a type of positive reinforcement metastable phenomenon. As highlighted by [58], several types

of lock-in are observed in the real-world, including technological, institutional and carbon lock-ins. Clearly, understanding lock-in effects is important for policy considerations. For example, where there are competing technologies with some being more carbon efficient than others, consumers will be more likely to invest in the cheapest most common technology with the most infrastructure than the one that is better for the environment [34].

In some regions of parameter space lock-ins occur in the model of Brock and Durlauf, where there are 2 possible lock-in states m^*: the optimal one where $\text{sign}(m^*) = \text{sign}(F)$, and the non-optimal one where $\text{sign}(m^*) = -\text{sign}(F)$, *which occur since the agent-to-agent interaction terms become dominant over the zeitgeist, i.e., switching to the alternate technology punishes the utility of an agent due to the collective effects.* However, whether a lock-in is observed or not depends on several factors. First, one must be in the regime wherein agents are rational enough to begin coalescing on either of the two choices, i.e., $\beta > \beta_c$. In this sense, β_c is not only a property of the steady-state but also a requirement for certain types of transient phenomena. Second, F should not be of too great a magnitude such that only 1 equilibrium solution of m is present (see Sec. 4 in S1 File). Thirdly, the initial condition should not be entirely weighted towards the steady-state distribution one finds as $t \to \infty$, i.e., since lock-ins are a path-dependent phenomenon there must be a viable opportunity for them to occur.

In many complex systems metastability occurs, and it requires a time-dependent analysis of the problem at hand, since since considering only the steady-state is no longer sufficient. In many cases this makes analytical treatment very difficult since time-dependent problems are rarely soluble. However, in this case we do have a solution, and in the sections that follow we proceed analytically. In the next section we derive the relaxation time scales to the steady-state for systems exhibiting lock-ins by determining the switching times between the two lock-in states. In the following section we will often refer to decisions as technologies, in line with the technology application drawn above.

3.2 Escape from non-optimal decisions

3.2.1 Relating the relaxation time scale to the first passage time. We now look at the lock-in mechanism in more detail using our analytical solution. The general case of metastability in bistable systems is covered by van Kampen [31], who does so in three steps. These steps are vital to the explanation of the lock-in mechanism, and in determining the relaxation time scale λ_2^{-1} to the steady-state as $t \to \infty$. Step 1 describes the evolution of the initial distribution. For $t \gtrsim 0$, the distribution broadens and probability modes have not yet developed at the equilibria. This is seen in Fig 2(a) for the distribution in red at $t = 0.1$ (the initial condition at $t = 0$ being that of equal numbers of agents deciding left and right). Step 2 is that two distinct modes have developed in $P(m(n), t)$, which decompose into left and right parts respectively. How the distribution has decomposed is dependent on the initial condition and can be seen in Fig 2(a) for the distribution in green. Finally for $t \gg 1$, step 3 is that each mode has developed its *local equilibrium shape* and that the transfer of probability between the modes becomes very small. This is shown in Fig 2(a) for the blue distribution and for the black dots, showing that the distributions between $t = 10$ and $t = 10^{10}$ are indistinguishable. At times $t \gg \lambda_3^{-1}$, where λ_3 is the third smallest eigenvalue of the master operator in Eq (15), the process can then be effectively modelled as a two-state process between the equilibria, with very small rates of probability transfer between the modes, as illustrated in Fig 2(d). In the following our main interest is in finding these rates of transfer between the behavioural modes and the overall rate of relaxation towards the steady-state.

Before proceeding, we illustrate how to calculate the equilibria values of m, including the unstable one, via the steady-state distribution alone (see Fig 2(b)). For $\beta > \beta_c$, the stable
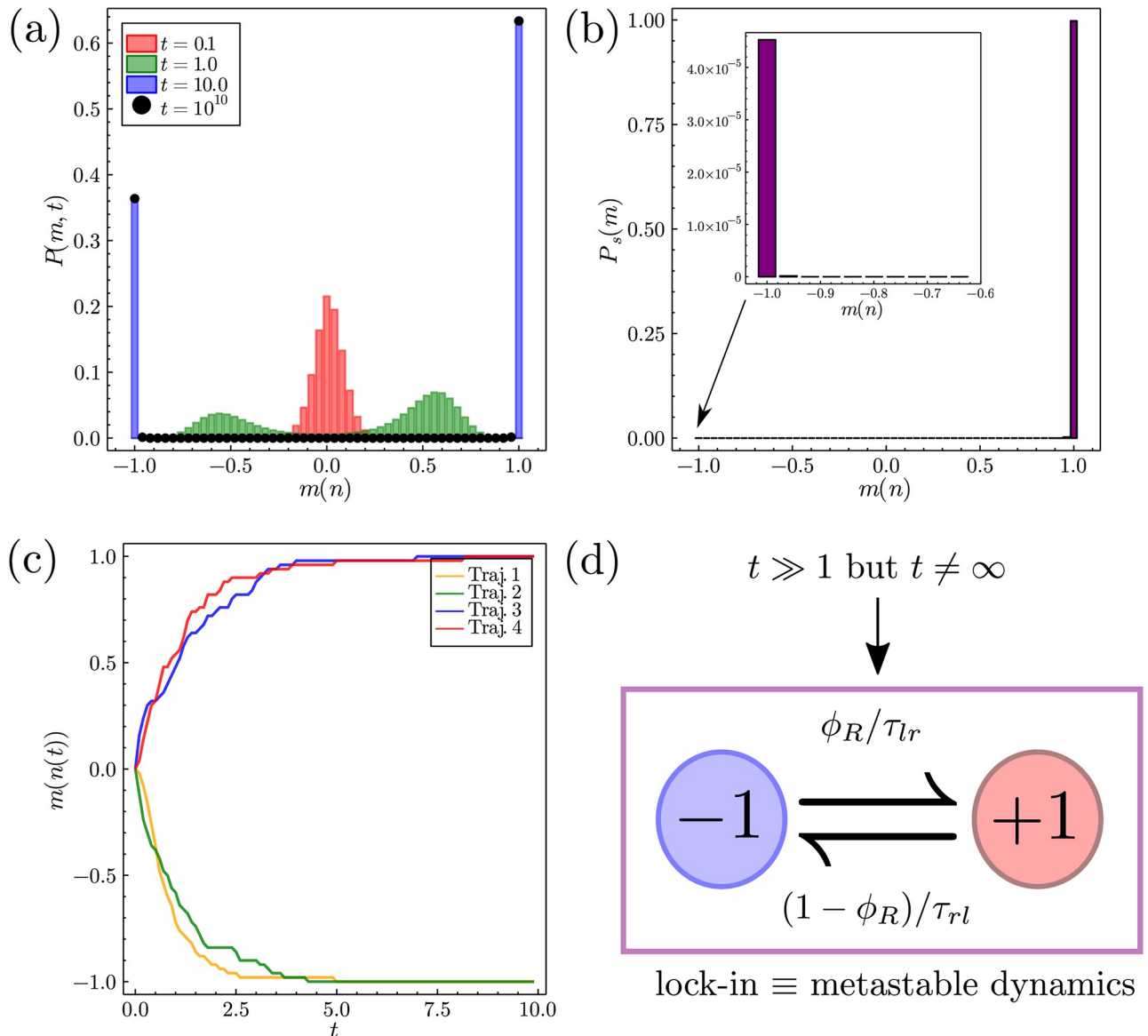
Fig 2. Plots showing the lock-in phenomena in the mean-field model. (a) For $F > 0$ and $\beta > \beta_c$ we show the evolution of the probability distribution given by Eq (16) from an initial condition at $n = N/2$. Beyond the initial condition we see the emergence of two modes of behaviour, the agents either increasingly choose the left or the right technology. The evolution of the probability distribution becomes very slow for $t > 10$ and the distribution at $t = 10^{10}$ is indistinguishable from that at $t = 10$. (b) A plot of the analytic steady-state distribution from Eq (22) shows that in the true steady-state limit almost all the agents will be locked into the right technology. Importantly, this is completely distinct from the time-dependent solution even at large times. Note the presence of a small mode at the unfavoured left-hand technology seen in the inset. (c) Individual SSA trajectories for the system showing the lock-in effect on individual populations. (d) As $t \gg 1$ the dynamics of the system becomes metastable and can be approximately mapped to a two state process with very small transition rates. Parameters for plots in this figure are $F = 0.1$, $J = 5$, $\alpha = 0$, $\beta = 1$, $\gamma = 1$ and $N = 50$.

equilibria m_- and m_+ are the maxima of the steady-state distribution (-1 and 1 in Fig 2(b)) with the larger of the two modes being the optimal equilibrium value. The intermediate unstable equilibrium point m_u is the minima of the distribution (found at $N/2$ for Fig 2(b)), and a system found either side of m_u will likely drift towards the corresponding stable equilibrium point. We will denote the critical *number* of right deciding agents as $n_u = N(m_u + 1)/2$. Note

that for $\beta \leq \beta_c$ (see Sec. 4 in S1 File), or for $|F| > J(\alpha + 1)$ in the $\beta \gg 1$ limit (see Sec. 6 in S1 File), there is only one equilibrium value of m.

Defining $\pi_L(t) = \sum_{m<m_u} P(m,t)$ and $\pi_R(t) = \sum_{m>m_u} P(m,t)$ as the probabilities to be in the left and right modes respectively, following the approximative two-state process in Fig 2(d), we can then assert that,

$$\partial_t \pi_L(t) = -\partial_t \pi_R(t) = -\frac{\phi_R \pi_L(t)}{\tau_{lr}} + \frac{(1-\phi_R)\pi_R(t)}{\tau_{rl}}, \tag{23}$$

where τ_{lr} and τ_{rl} are the mean times to escape the from equilibria at the left and right modes respectively (i.e., starting at the equilibria, how long it takes to reach m_u), and ϕ_R is the probability that if the system starts at $m(0) = m_u$ that the agents initially coalesce on the right technology. We derive ϕ_R in Sec. 5 in S1 File (using similar methods as the calculation of the mean first passage time in the next section). This probability enters the rates of transition to the other mode since τ_{lr} and τ_{rl} only give the times to escape from each mode, which must be scaled by the probability to enter the other mode, since upon reaching m_u the agents could also revert back to the decision they inhabited before. Eventually, π_L and π_R reach their stationary values which are determined by $\partial_t \pi_L^s = 0$, explicitly,

$$\frac{\pi_L^s}{\pi_R^s} = \frac{\tau_{lr}(1-\phi_R)}{\tau_{rl}\phi_R}. \tag{24}$$

This equation helps us interpret the results of Fig 2(b): for the chosen parameter set $\tau_{lr} \ll \tau_{rl}$: once the agents have made the optimal decision they will not change it on any reasonable time scale. Note that even at the steady-state there is a mode at $m = -1$ (see inset Fig 2(b)), and that the *shape* of the left-hand distribution will be near identical to the shape of the distribution at $t = 10$ in Fig 2(a), but is of much smaller magnitude. The three steps described by van Kampen can also be seen on a SSA trajectory level in Fig 2(c): after an initial period of indecisiveness the individual population trajectories eventually coalesce on either the optimal technology at $m = 1$ (with slightly greater probability) or else the sub-optimal technology at $m = -1$.

Before calculating the switching times between the equilibria, one can ask how these switching times are related to the rate of relaxation to the steady-state. Namely, how do τ_{lr} and τ_{rl} relate to the smallest magnitude non-zero eigenvalue λ_2? We know that for $t \gg \lambda_3^{-1}$ the only relevant time scale is the relaxation time scale from the metastable state to the steady-state, hence we can write,

$$P(m,t) \sim P_s(m) + \exp(-\lambda_2 t)\Phi_2(m), \tag{25}$$

where $\Phi_2(m)$ is the eigenvector of $\mathbf{A}$ (see Eq (15)) corresponding to the eigenvalue λ_2. Inserting Eq (25) into Eq (23) we find that,

$$\lambda_2 \sim \frac{\phi_R}{\tau_{lr}} + \frac{(1-\phi_R)}{\tau_{rl}}, \tag{26}$$

where we have used the fact that $\sum_m \Phi_2(m) = 0$, which comes from summing Eq (25) over all m and enforcing normalisation conditions on $P(m,t)$ and $P_s(m)$. As Bouchaud showed in [3], one can approximate the master equation in (14) as a Fokker-Planck equation [31, 43], hence

finding that the mean first passage times are proportional to

$$\tau_{lr} \propto \exp(N(1 - F/J(1+\alpha))), \tag{27}$$

$$\tau_{rl} \propto \exp(N(1 + F/J(1+\alpha))), \tag{28}$$

whose full derivation we show in Sec. 6 in S1 File. The utility of this result is its ease of interpretation: where there are two stable equilibria the mean times for switching between them are *exponential in the number of agents*.

3.2.2 A better approximation of the relaxation time scale. Eqs (27) and (28) are very good approximations in the $\beta \gg 1$ and $N \gg 1$ limits where $m_{\pm} = \pm 1$. However, there are some cases where the distributions $\pi_L(t)$ and $\pi_R(t)$ have a greater variance and are less peaked (as illustrated in Fig 3(a)) in which case contributions to the time needed to pass the potential barrier at m_u must be taken from multiple values of m. We first define the conditional normalised probability distributions of having m inside each of the the metastable phases as $\rho_l(m < m_u) = P_s(m)/\sum_{m<m_u} P_s(m)$ and $\rho_r(m > m_u) = P_s(m)/\sum_{m>m_u} P_s(m)$ for the left and right equilibria respectively. We determine this from the intuition that the metastable probability modes are the same as those found in the steady-state distribution up to a multiplicative pre-factor, an intuition that we confirm in Fig 3(b). One can then define the mean times to switch between the two equilibrium modes at $m < m_u$ and $m > m_u$ as weighted sums over the conditional distributions,

$$\tau_{lr} = \sum_{n=0}^{n_u-1} \rho_l(m(n))\tau_n, \tag{29}$$

$$\tau_{rl} = \sum_{n=n_u+1}^{N} \rho_r(m(n))\tau_n, \tag{30}$$

where τ_n is the mean first passage time to reach n_u given one starts with n agents deciding on the right-hand technology. In our case it is possible to find the values of τ_n *exactly*, and we do so in line with methods shown in [31, 59, 60].

Consider again the microscopic transitions previously seen in Fig 1(b). For this birth-death process one can write a *backward equation*, which is formally the adjoint equation to the master equation, commonly used for first passage processes. For our purposes, it is more convenient to use the discrete time backward equation given by [31, 59],

$$Q_{j,i}(t + \Delta t) = a_{i+1}\Delta t Q_{j,i+1}(t) + b_{i-1}\Delta t Q_{j,i-1}(t) + (1 - (a_{i+1} + b_{i-1})\Delta t)Q_{j,i}(t), \tag{31}$$

where $a_i = (N - (i-1))r(i-1)$, $b_i = (i+1)l(i+1)$, $Q_{j,i}(t)$ is the probability of being found with j agents deciding on the right technology a period of time t after being found with i right technology deciding agents, and Δt is the time step (which is taken to zero in the continuous time limit). Note that the absolute time t_n at time step n is defined by $t_n = n\Delta t$.

The mean first passage times for hitting m_u from $m < m_u$ and $m > m_u$ must be considered separately. In the following we show the calculation for $m < m_u$, although the procedure is analogous for $m > m_u$. Consider only the states of the system $m(n) < m_u$, where we define $m_u = m(n_u)$ with n_u being the number of agents deciding for the right technology at the unstable equilibrium point. We define a new Markov process by setting $b_{n_u-1} = 0$, which defines m_u as an absorbing boundary [18, 31]. A schematic of these new dynamics is show in Fig 3(c). From the backward equation for this new process we then define $\psi_i(t) = Q_{n_u,i}(t)$ as the *cumulative probability of reaching n_u a time t after having i right deciding agents. Hence, the probability
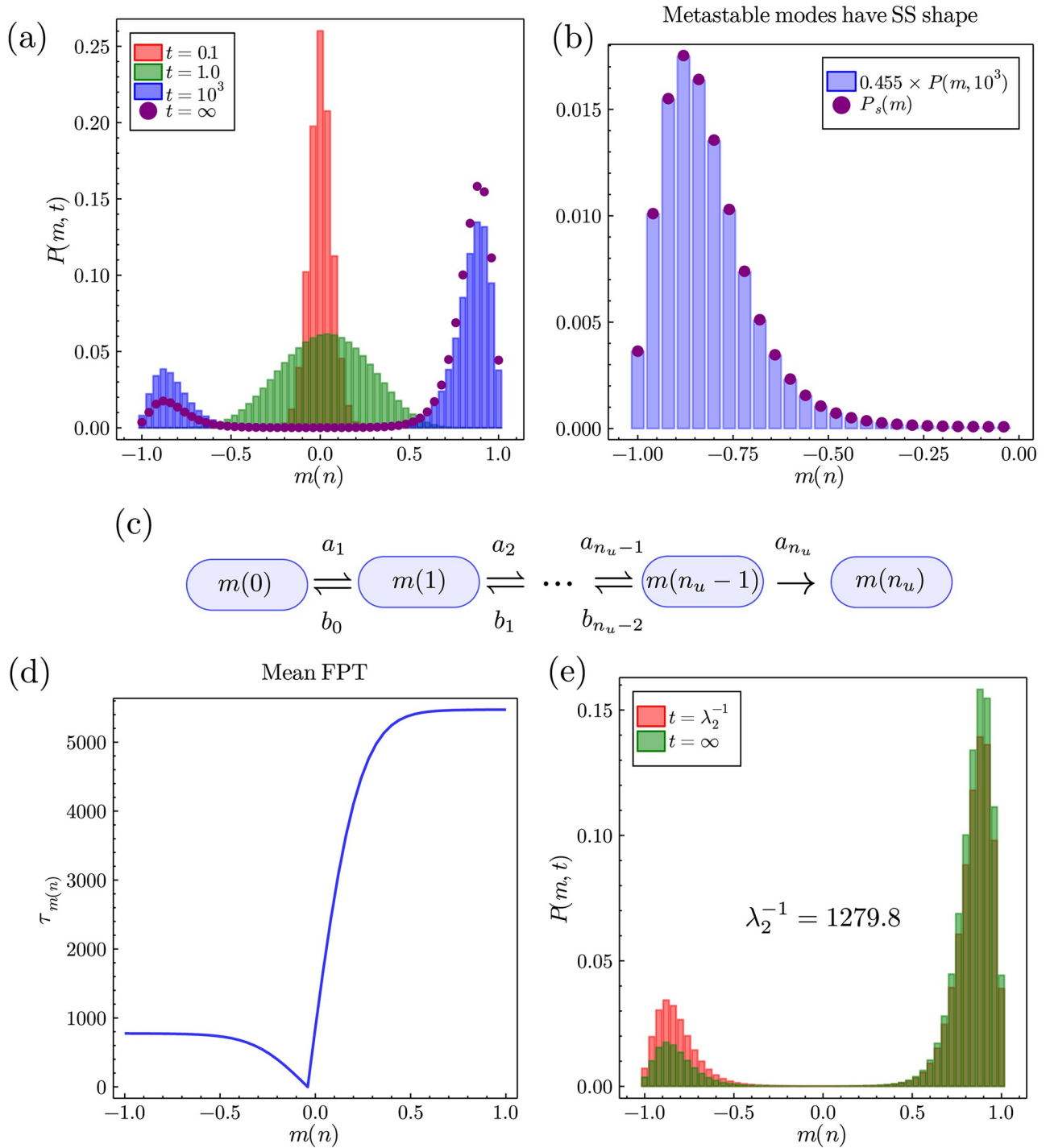
Fig 3. Figure showing the coalescence of the agents onto stable equilibria where the modes are not found at $m = \pm 1$ and fluctuations are present, for parameters $F = 0.025$, $J = 1.5$, $\alpha = 0$, $\beta = 1$, $\gamma = 1$ and $N = 50$ using the analytic solution from Eq (16). (a) Plots of $P(m, t)$ at times from near the initial condition at $m = 0$ to the steady-state. Note that for $t \gtrsim 3 \times 10^3$ the time-dependent solution becomes indistinguishable from the steady-state. (b) Plot showing that the metastable modes have the same *shape* as the modes of the steady-state distribution. We show that the right-hand mode rescaled by a pre-factor (= 0.455 here for $t = 10^3$) becomes indistinguishable from the steady-state distribution. (c) New dynamics considered for the calculation of the mean first passage time τ_{lr}. Note that a similar, but separate, diagram can be drawn for the calculation of τ_{rl}. (d) Plot of the mean first passage time to reach m_u given one starts at $m(n)$. It is clear that since $F > 0$ the mean first passage times to hit m_u are greater for $m > 0$. (e) Plot of the time-dependent distribution at $t = \lambda_2^{-1} = 1279.8$ (using our approximation) versus the steady-state distribution.

of hitting n_u at time t is given by $\psi_i(t) - \psi_i(t - \Delta t)$, and the mean first passage time τ_n is given by a weighted sum over these probabilities,

$$\tau_n = \sum_{i=0}^{\infty} i\Delta t(\psi_n(i\Delta t) - \psi_n((i-1)\Delta t)), \tag{32}$$

with $\psi_n(-\Delta t) = 0$. From the backward equation we find the recursive relationship for $\psi_i(t)$,

$$\psi_i(t + \Delta t) = a_{i+1}\Delta t\psi_{i+1}(t) + b_{i-1}\Delta t\psi_{i-1}(t) + (1 - (a_{i+1} + b_{i-1})\Delta t)\psi_i(t), \tag{33}$$

which has the intuitive interpretation that the probability of reaching m_u at time $t + \Delta t$ is the probability of hopping to $i+1$ and reaching m_u from there, *plus* the probability of hopping to $i-1$ and reaching m_u from there, *plus* the probability of not hopping and reaching m_u from i [59]. If we subtract $\psi_i(t)$ from both sides of Eq (33), multiply by t, and sum over all t we then get a recursion relation for the mean first passage time,

$$a_{i+1}\tau_{i+1} + b_{i-1}\tau_{i-1} - (a_{i+1} + b_{i-1})\tau_i = -1. \tag{34}$$

One can perform similar calculations for the higher order moments of the first passage time distribution, although we do not consider them here (see [59] for more details). We have two boundary conditions on this recursion relation. The first is $\tau_{n_u} = 0$, which reflects the fact that if one starts at n_u the time taken to reach it is obviously 0. The second is less obvious in that it comes from physical conditions at the left boundary and is $\tau_1 - \tau_0 = -1/a_1$. This reflects the fact that in the state $n = 0$ there is only one possible move to $n = 1$, which occurs with average time $1/a_1$. Now, we introduce the difference variable $\eta_i = \tau_i - \tau_{i-1}$ which transforms Eq (34) into,

$$\eta_i = \frac{b_{i-2}}{a_i}\eta_{i-1} - \frac{1}{a_i}, \tag{35}$$

subject to $\eta_1 = -1/a_1$. This can be solved recursively and the result is,

$$\eta_i = -\sum_{j=1}^{i} \frac{1}{a_j}\prod_{k=j}^{i-1} \frac{b_{k-1}}{a_{k+1}}, \tag{36}$$

where again we note that the empty product is equal to 1. Finally, to find the τ_n from η_n we see that,

$$\tau_{n<n_u} = -\sum_{i=n+1}^{n_u} \eta_i = \sum_{i=n+1}^{n_u}\sum_{j=1}^{i} \frac{1}{a_j}\prod_{k=j}^{i-1} \frac{b_{k-1}}{a_{k+1}}, \tag{37}$$

where we have used the fact that $\tau_{n_u} = 0$. Using the same approach (or via symmetry considerations) one can derive the case of $n > n_u$, whose result is,

$$\tau_{N-n>n_u} = \sum_{i=n+1}^{N-n_u}\sum_{j=1}^{i} \frac{1}{b_{N-j}}\prod_{k=j}^{i-1} \frac{a_{N-(k-1)}}{b_{N-(k+1)}}. \tag{38}$$

The results derived in Eqs (37) and (38) are *exact*. If one wishes for a simpler result, it is possible to simplify the expressions in the large N limit by approximating the product term in Eqs (37) and (38) with $\prod_k \gamma_k(n) = \exp(\sum_k \log(\gamma_k(n))) \sim \exp(N \int \log(\gamma_k(n))dn)$, where we have explicitly included the dependence on n for clarity (see [60] for more details). Doing so gives similar exponential dependence on N as we explored in Eqs (27) and (28), and hence we do not show the result of the large N approximations on Eqs (37) and (38) here.

We show a plot of $\tau_{m(n)} \equiv \tau_n$ in Fig 3(d) for $F > 0$, where we clearly see that it is more difficult to escape from the optimal choice technology than the sub-optimal since on average one has to wait much longer to escape the more optimal collective decision. The values of τ_n determined via Eqs (37) and (38) can then be used in combination with Eqs (29) and (30) in order to find the relaxation time scale λ_2 in Eq (26). Note that although this determination of λ_2 is still formally an approximation it is very accurate, and we show in Fig 3(e) that for the time-dependent solution at $t = \lambda_2^{-1}$ it results in a distribution very close to the steady-state distribution. Computationally, using `eigvals`, we find $\lambda_2^{-1} \sim 1288.8$ for Fig 3, whereas our approximation gives $\lambda_2^{-1} \sim 1279.8$, hence only slightly underestimates the relaxation time to reach the steady-state. Our approximation is an underestimation since the relaxation time since it does not take into account the initial relaxation into the metastable state of $\mathcal{O}(\lambda_3^{-1})$.

Since for Fig 3 we have $N = 50$ agents, one can also conclude that our method works well *even when not in the large N limit*. Moreover, our approximation is even better for systems such as that seen in Fig 2, where the modes at n_- and n_+ are very strongly peaked, since this type of system more closely corresponds to the approximations we have made in our calculation of λ_2 as the time taken to reach the metastable regime is even shorter compared to the time taken to reach the steady-state. The disparity seen between our approximation for λ_2 for the parameters in Fig 3 constitutes a worst case scenario of the calculation of λ_2. Eq (25) then constitutes an approximate solution for the bimodal regime of the mean-field model that does not require calculation of the fast decaying eigenvalues computationally, valid where $t \gg \lambda_3^{-1}$. We finally observe that our calculation of λ_2 gives us an approximate time-dependent probability distribution, $P(m, t) \sim P_s(m) + \exp(-\lambda_2 t)\Phi_2(m)$, *which does not require the calculation of any eigenvalues and is computationally valid in the metastable regime where all other eigenvalues of order $\mathcal{O}(\lambda_3^{-1})$ or less have decayed away*. Practically, in order to implement this result, upon realising that we have $\lambda_1 = 0$ and λ_2 we then substitute these into Eq (16) and where $t \gg \lambda_3^{-1}$ we can safely ignore the contributions from $i \geq 3$ in the sum.

4 Model calibration

Brock and Durlauf [1] used their equilibrium solution for econometric analysis and model calibration. However, as we have emphasised in the previous section, an equilibrium solution is often not applicable on any realistic time scale, even for small numbers of agents, and hence time-dependent dynamics of the binary choice model must be considered. Generally speaking, finding an analytic time-dependent likelihood function for an agent-based model is a rarity [25], however our time-dependent solution for the probability distribution allows us to construct one for the mean-field binary decision model, *allowing us to conduct practical model calibration in a short time*. This makes our solution useful to researchers who do not have access to vast amounts of computing power. We then test our calibration procedure on simulated data with known parameters in order to assess the conditions on the data necessary to provide reliable calibration.

4.1 Construction of likelihood function

We begin by defining the likelihood in the standard way. Say we have a set of L data points $\mathcal{M} = \{m(t_i)\}$ for $i \in \{1, 2, \ldots, L\}$, measured at times $\{t_1, t_2, \ldots, t_L\}$ describing the evolution of the order parameter $m(n(t))$ over some time period. In general one cannot assume this process is at equilibrium and the evolution from the initial condition at $m(t_1)$ does not follow a steady-state trajectory. This requires us to use Eq (16) in order to calculate the *probability of observing the trajectory $\mathcal{M}$ given some assumed parameter set $\theta = \{F, J, \gamma\}$, known as the likelihood*, and is

given by,

$$L(\mathcal{M}|\theta) = \prod_{i=1}^{L} P_\theta(m(n(t_i)))$$

(39)

where $P_\theta(m(n(t_i)))$ is Eq (16) evaluated for parameter set θ at time t_i. The likelihood function is expressed as a product of probabilities over the whole time series since it is the probability of observing $m(t_1)$ at t_1 *and* $m(t_2)$ at t_2 and so on (hence from the laws of probability is multiplicative). Note that since β pre-multiplies F and J and $(1 + \alpha)$ pre-multiplies βJ in the utility function, β or α cannot be inferred separately but only βF and $\beta(1 + \alpha)J$ can be inferred [1]. Hence for calibration we set $\beta = 1$ and $\alpha = 0$ and infer only F, J and γ. The aim of the calibration procedure is then to find the parameter set $\theta^\star$ that maximises $L(\mathcal{M}|\theta)$ with respect to θ. Generally, since the likelihoods are generally very small quantities, it is more computationally convenient to instead minimise the negative log likelihood $-\ln(L(\mathcal{M}|\theta))$ which generally takes values $\gg 1$. In most cases (including ours), the parameter set corresponding to the minimum value of $-\ln(L(\mathcal{M}|\theta))$ cannot be analytically determined and hence one must proceed algorithmically by testing many different values of θ via an optimisation algorithm. In this paper we utilise the *adaptive differential evolution* optimiser from the Julia package `BlackBoxOptim` [61, 62], which is determined to be the best likelihood optimisation algorithm compared to several other state-of-the-art methods [62]. Using this algorithm, the optimal parameter set $\theta^\star$ is then determined through,

$$\theta^\star = \underset{\theta \in \Theta}{\arg\min}(-\log L(\mathcal{M}|\theta))$$

(40)

where Θ is the set of all possible parameters in the optimisation range selected. In the calibration that follows the true parameter set for the simulated data is $\theta_{\text{true}} = \{F = 0.025, J = 1.5, \gamma = 1.0\}$ (same as in Fig 3) and the parameter ranges of optimisation for the set Θ were chosen such that $F \in [-2, 2]$, $J \in [\exp(-2), \exp(2)]$ and $\gamma \in [\exp(-1), \exp(1)]$, where parameters J and γ are optimised in log-space. For the purpose of analysing the errors in the calibration procedure below we define,

$$E_{tot} = \sum_i \left| \frac{\theta_{\text{true},i} - \theta_i^\star}{\theta_{\text{true},i}} \right|,$$

(41)

$$f = \left| \frac{(F_{\text{true}}/J_{\text{true}}) - (F^\star/J^\star)}{F_{\text{true}}/J_{\text{true}}} \right|,$$

(42)

where E_{tot} is the total error on the inference procedure and f is the error in the fraction between F and J. In most econometric analyses it will be the error in f which is most important since it tells us whether one has properly inferred the magnitude of the influence of exogenous versus endogenous effects on the agents. These error functions will then allow us to determine the conditions necessary of data such that one can conduct a valid model calibration. We note that $\theta^\star$ does not generally correspond the global minimum of $-\ln(L(\mathcal{M}|\theta))$, but instead a *good local minimum*. This is due to the complexity of the function $-\ln(L(\mathcal{M}|\theta))$, a problem for which there is no known solution to produce the global optimum in a reasonable computational time [63]. The number of optimisation steps we choose for the adaptive differential algorithm is 500, with a population size of 1000 such that each calibration procedure took less than 1500s on a laptop with Intel Core i7–8650U CPU 1.90GHz x 8 running Ubuntu 18.04.5 LTS.

4.2 Calibration from a single trajectory

In many real-world situations data is only collected once for a particular event. For example, national elections do not have multiple realisations, hence if one was to collect the data of the percentage of votes for Democrats or Republicans at all elections from 1868 (from when only Democrats *or* Republicans have won the presidential vote) then one ends up with a single trajectory of data. Therefore, it is important to assess the conditions under which calibration procedures are accurate with respect to data for which the parameters are known. For this purpose we utilise the SSA to provide stochastic trajectories for a particular realisation of our mean-field system for the parameter set explored in Fig 3, which notably expresses bimodality.

First, we look at the case of calibration where only one of the two equilibria is explored, from the trajectory seen in Fig 4i(a). The question here is: is there enough information in a single trajectory (from a bimodal system) exploring a single equilibrium mode for the correct parameters to be inferred? The answer is no, which can be seen from a plot of the errors in the inference against the calibration time (for a fixed number of 100 data points) used for the inference in Fig 4i(b) and 4i(c). Even though increasing the calibration time improves the calibration, the overall inference of the parameters is still poor for large calibration times with the errors being $\gg 1$. The reason for this is simple: for a system that expresses bimodality the probability is shared across both modes, hence for a trajectory that only realises one of its two equilibria in a given realisation, the optimiser will instead choose a set of parameters $\theta^\star$ that corresponds to the single mode explored in the data.

Having ruled out the ability to conduct good optimisation when only a single equilibria is explored, we now look at the case where a system realises both of its modes of behaviour on a given trajectory, shown in Fig 4ii. The trajectory for this realisation is shown in Fig 4ii(a), where the mode of behaviour changes approximately half way through the trajectory. As seen from Fig 4ii(b) and 4ii(c), the calibration is significantly improved when both equilibria are explored in the calibration procedure (using a fixed number of 100 data points as before). The reason for this is relatively clear: parameter sets for which the probability distribution exhibits only a single mode near $m = -1$ or 1 have a lower likelihood, when the system explores the opposite mode from the one they describe. Hence, one can conclude that if the system is bimodal, and the data expresses both of these behaviours, the calibration produced will be relatively good.

Finally, one may want to know the optimal number of data/time points to use, rather than the optimal time of calibration. Fig 4iii(a) shows the cases of calibration using differing numbers of data points over the entire trajectory considered in Fig 4ii(a), from 1001 to 10 data points. Fig 4iii(b) and 4ii(c) show the results of inferring the parameters with respect to the errors E_{tot} and *f*: one observes that having more data points is better, but recognises diminishing returns with the additional data points beyond around 10^2. Therefore, having more data points generally leads to a better parameter estimate but is not as important as having data that represents all behavioural modes of a given parameter set.

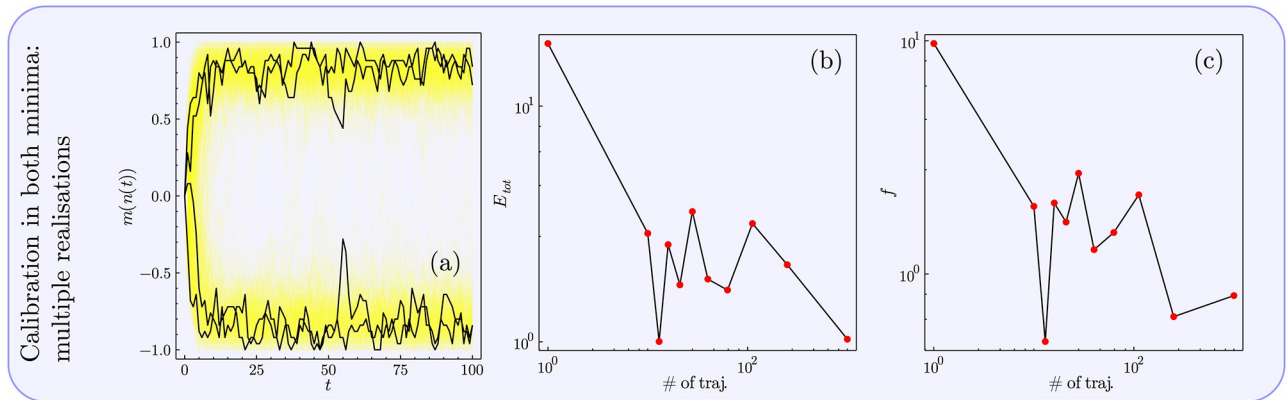## 4.3 Calibration from multiple trajectories

On some occasions there exist socio-economic binary decisions with more than one realisation. For example, although American presidential elections only happen once every four years, prior to the elections pollsters survey the public to assess what the current opinion is [64]. *These multiple surveys across the different elections constitute different independent realisations of the same socio-economic phenomena*, if one excludes pollster bias or the possibility that over different elections the underlying model parameters are different. Hence, having multiple realisations of the same phenomena does not mean the existence of multiple realities, but
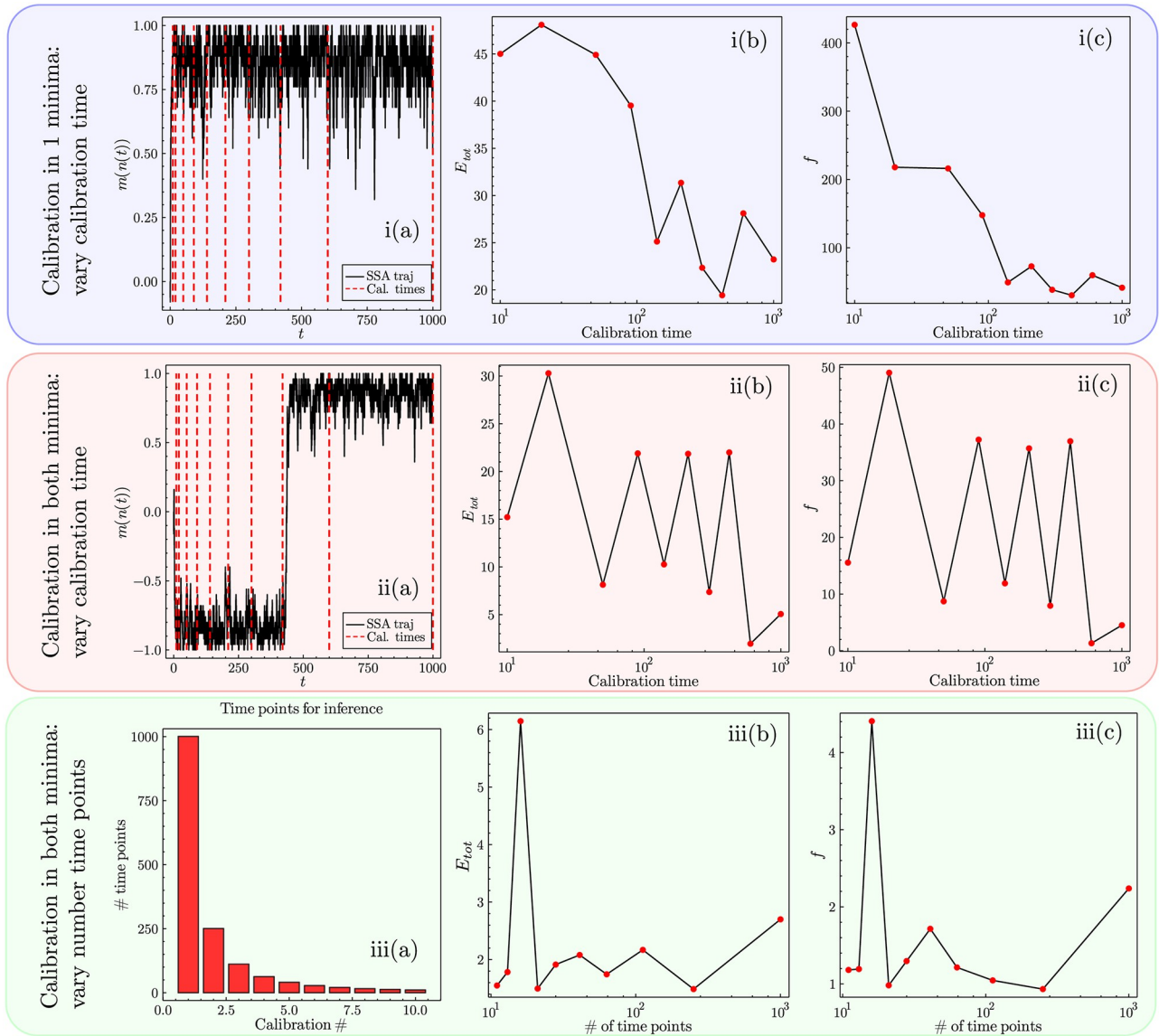
Fig 4. Figure showing the calibration procedure on a single trajectory/realisation of data produced by the SSA for the parameter set explored in Fig 3. (i) Exploring the calibration when only one equilibrium of the two is realised on the data trajectory. i(a) The data which we perform the calibration on, clearly showing that only the right-hand equilibrium is manifest. Red dashed lines show the various times used for calibration. In i(b) and i(c) we explore the various calibration times and plot the error on the calibrated parameters compared to the true values for E_{tot} and f respectively defined in Eqs (41) and (42). Although larger calibration times result in better parameter inference there are still large errors $\gg 1$ even for large calibration times. (ii) Exploring the calibration procedure for a trajectory that realises both equilibria. ii(a) The trajectory that we use for calibration that explores both equilibria. ii(b) and ii(c) show that increasing the calibration time such that the exploration of both equilibria occurs results in much improved inference of the parameters where for calibration times $\sim 10^3$ the errors are of order $\mathcal{O}(1)$. (iii) Exploring the trajectory in ii(a) for a varied number of time/data points. iii(a) Bar chart showing the different number of time points explored in the calibration. iii(b) and iii(c) show that although having an increased number of time points benefits calibration, it does so with diminishing returns. Note throughout the figure that the optimiser used from `BlackBoxOptim` generally identifies good *local minima* of the likelihood function and not the global minimum due to the complexity of the likelihood function [62].

simply temporally or spatially separated independent events which one assumes have similar exogenous and endogenous influences on the agents. Having different realisations can be very beneficial for the calibration procedure, since as we saw for the case of a single trajectory, if only one behavioural mode is explored the calibration is weighted towards parameter sets that

Fig 5. Figure showing the performance of the calibration procedure when one has access to multiple realisations of a binary decision process. (a) We simulated 10^3 trajectories of binary decision data from the SSA for the parameter set used in Fig 3. We emphasise five possible trajectories in the foreground, with the yellow background giving an idea of all the trajectories we used. (b) and (c) show that the model calibration can be significantly improved if one has access to multiple realisations of the same binary decision process. For $> 10^2$ realisations we find that the errors are typically ≤ 1, which corresponds to a very accurate calibration.

https://doi.org/10.1371/journal.pone.0267083.g005

favour that reality. Note that the example we explore the initial condition is fixed and the independent trajectories have exactly the same underlying parameter sets (in reality there would be some variations in *F*, *J* and γ between the independent events). However, it shows the considerable effect that multiple realisations have on model calibration.

In Fig 5(a) we show 1000 realisations of the process for the parameters in Figs 3 and 4 (in yellow), highlighting five of the trajectories (in black). Fig 5(b) and 5(c) show that for an increased number of realisations the error in the calibration is much reduced, for both E_{tot} and *f*. This reduction in error is even more pronounced than the reduction due to increased calibration times or number of data points seen in Fig 4. The reason for this is that if one has multiple trajectories of the same process then it is much more likely that both equilibria will be explored, *and also that the number of trajectories that explore each equilibria is proportional to the probability that a single trajectory will be found in that state.*

In summary, we find that there are several conditions on data that can result in more accurate model calibration, which are:

1. If the system can express bimodal behaviour, and one only has a single data trajectory, then it is imperative that the trajectory used explores both of these behavioural modes. If this is not the case the calibration procedure will weight itself towards parameter sets that only realise the behaviour seen in the data.

2. Having a longer calibration time, or an increased number of data points, both improve the accuracy of the calibration, but *with diminishing returns*.

3. Having access to more than one realisation of the situation one wishes to model is highly beneficial and results in very accurate calibration. This is seen in Fig 5(b) and 5(c) where the number of trajectories exceed approximately 10^2. Note also the sizeable drop in error (in log-scale) from a data-set with one realisation to a data-set with 11 realisations in both of these figures. We stress that from a single realisation of real-world data one does not know *a priori* whether the system expresses bimodality, hence having multiple realisations can be very informative, and provide for much better calibration.

4.4 Other methods for model calibration

Although it is very convenient for us to utilise the likelihood function based on our time-dependent solution, other likelihood-free calibration methods are available. One of particular mention is *approximate Bayesian computation* (ABC), which generates SSA (Monte Carlo) trajectories for a given parameter set θ which can then be compared to the original data using a distance function [65, 66]. The choice of distance function is important, and typical examples include the Euclidean distance between the trajectories, the Hellinger distance, or even the Wasserstein distance [67]. Often it is best to experiment with each of these, or combinations of them, to see empirically which gives the best result from simulated data, before applying the calibration procedure to a real-world data-set.

5 Neoclassical economics versus the binary decision model

In this section we compare the results of the paper to the tenets of neoclassical economics (NCE), and in particular explore: (i) information and expectations, (ii) the dichotomy between the social planner and altruistic agents, and (iii) the implications of our findings on model calibration to economics. Note that many of the points we make here are not first noted by us, and one may additionally want to read further publications such as [3, 6, 37, 39, 68–70] which have inspired this author.

5.1 Information and expectations

NCE assumes that agents have perfect rationality in the sense that all agents can instantaneously perform simultaneous complex calculations and arrive immediately at an equilibrium based on a total knowledge of present and future [39]. However, in the binary decision model no two agents make a decision at the same time, and the maximum foresight an agent can have is to choose the decision that maximises the agent's utility *at that point in time*. There is no capacity for the model agents to look into the future, or else to gain an insight into which technology is the optimal one, and hence lock-ins still occur within the binary decision model even where agents are 'perfect' (in the limit $\beta \to \infty$). This would not occur in a neoclassical model as the agents would all decide to choose the optimal technology in order to maximise their individual utilities.

5.2 Social planner versus altruistic agents

In NCE the ideas of having selfish agents and a social-planner/auctioneer go hand-in-hand. However, in the binary decision model we have explored, the 'social planner' situation more closely corresponds to a system of altruistic agents of altruistic strength $\alpha = 1$ rather than the system of selfish agents, since the altruistic agents at least consider how each agent can change to best affect the global utility. This dichotomy is curious, since from the perspective of our agent based model the social planner and selfish agents cannot co-exist.

As Bouchaud noted in [3], the papers of Grauwin et al. [42, 71] are remarkable in that they exhibit situations in which selfish agents fail spectacularly in a Schelling-like global coordination problem, breaking Adam Smith's 'invisible hand', whereas having agents that are even somewhat altruistic remedies the situation for the benefit of all agents. One can further ask a similar question for the mean-field binary decision model: does having altruistic agents increase the ability of the population to increase global utility? The answer to this question is mixed. In one sense the answer is yes—increasing α increases the endogenous influence and hence the time taken to coalesce on a single decision in the population is much reduced. Additionally, in each behavioural mode the fluctuations are reduced if agents are altruistic, shown
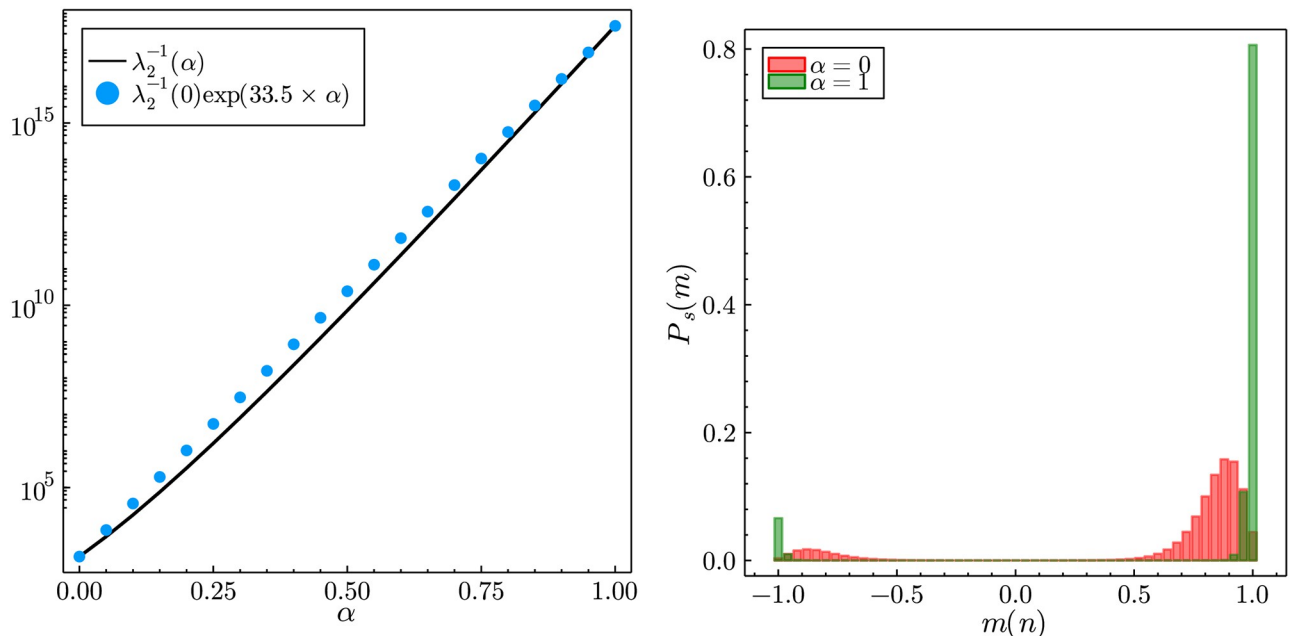
Fig 6. For the set of parameters explored in Fig 3 we explore how the metastable relaxation times (using our very accurate approximation) and the equilibrium distribution behave with respect to changing agent altruism. The left-hand plot shows that as agent altruism increases the metastable waiting times (black line) become exponentially large in α. The blue dots show an exponential approximation to λ_2^{-1}, clearly exhibiting its close-to-exponential behaviour. The right-hand plot shows the change in the equilibrium ($t \to \infty$) distributions. For increasing agent altruism populations become more polarised in each behavioural mode (with much reduced fluctuations) even in the metastable regime.

https://doi.org/10.1371/journal.pone.0267083.g006

in the right-hand plot in Fig 6, decreasing global utility compared to selfish agents. However, in another sense the answer is no—altruistic agents do not know *a priori* which technology, left or right, is the optimal one and hence can easily coalesce on the wrong technology. In the situation where this occurs the waiting time for them to leave the non-optimal decision is much greater than the selfish agents (shown on the left of Fig 6), and in fact the waiting time to equilibrium is roughly exponential in α. Hence as Brock and Durlauf [1] state, altruistic agents are more susceptible to conformity effects; *however, their ability to reach the optimal equilibrium mode often does not occur on a relevant time scale.*

5.3 Implications of calibration procedure

Previously in Section 4.3, we defined the conditions for good model calibration, which in essence were: many data points, long calibration times, and multiple trajectories. However, the opinion of some of the literature [25] seems to be that one of the main issues with model calibration lies in not having explicit likelihood functions. In our case, *even with an analytically defined likelihood function, and only three parameters to infer, model calibration is still a difficult task unless one utilises a well-informed data-set.* Additionally, as we have already commented, it is possible to conduct calibration without an explicit likelihood function using likelihood-free methods for parameter inference [66]. It is hence vital for model calibration that either calibration methods become much smarter, for example using methods beyond simply using a likelihood function as done in [72] (here in the context of gene expression), or else the data used for calibration becomes more informative. Although it was found that multiple data realisations are the biggest improvement that can be made to the inference procedure, in practise, for many questions of interest, it is not possible to access such data. Hence, the

need for quantities of good quality economic data is a pressing one since economists are already using such calibrated models for economic prediction. In lieu of such well informed data-sets with which to conduct econometric analysis, economists are limited to optimising their models for one of many indistinguishable parameter sets from the calibration of their models.

6 Conclusion

In this paper we have solved the binary decision model of Brock and Durlauf [1] in time by mapping it to a stochastic birth-death process which can be solved via the method of [44]. We explored the waiting times to the steady-state in the metastable regime using a very accurate method based on first passage time theory, and used the solution to construct the likelihood function for use in model calibration. The method we employed from [44] can also be used to solve Kirman's ant recruitment model in time [7, 10, 11]. We additionally note that our solution in Eq (16) is not only a solution to the binary decision model, but is also a time-dependent solution to the mean-field Ising model used as an approximate description of magnetic behaviour in physics. Previous time-dependent solutions to this problem have only come in the form of hydrodynamic approximations [73]. One of the main utilities of our solution is the ability to infer $\{F, J, \gamma\}$ from real economic binary decision data, and that these three parameters completely specify the dynamics of the agents (up to the choice in decision rule and multiplicative factors β and α). We constructed a likelihood function and showed that model calibration, even in our simple mean-field model, is a non-trivial task unless one has access to an informative data-set made up of multiple realisations of the same socio-economic phenomena.

Our solution provides a platform for several enhancements and investigations of the model, including:

1. An exploration of non-logit decision rules (such as the Arrhenius form), and additionally decision rules that break detailed balance. This can easily be done using our solution in Eq (16), since it is general in the form of the transition rates $W_n(S_i \to -S_i)$. The exploration of non-detailed balance decision rules is of particular importance, as emphasised by Bouchaud [3], since economies are not closed systems but are subject to energy influx/out flow. Recent publications indicate that breaking detailed balance results in system properties that are not consistent with properties of systems pertaining to detailed balance [74].

2. In this paper we have not explored our solution with respect to time-dependent $F(t)$ (whose solution is discussed in Sec. 2 in S1 File), in particular with the rise of metastable states. An understanding of how the time-dependence on $F(t)$ can affect metastability and lock-in effects would have relevance to policy makers, for example in affecting the transition to more renewable energy sources by reducing the time spent fixated in the non-optimal side of a technology lock-in. A question of interest would be: given a system of agents is in the lock-in state in the non-optimal technology, what is the optimal time-dependent function $F(t)$ that releases the agents from this lock-in (in minimal time) whilst keeping $\int_0^\infty F(t)dt$ to a minimum (i.e., reducing the effort necessary to break the lock-in)?

3. Developing methods to analytically solve multiple choice models, such as those explored in [2, 34]. These models are more generalised than the binary decision model we have discussed in this paper, and in fact contain the binary decision model as a special case, so solutions for multiple choice models would have more potential applications.

4. A more detailed investigation of model calibration using more realistic simulated data-sets and real world data-sets. Can one do better than the classic likelihood based inference using

more advanced methods? Additionally one could explore the performance of likelihood-free methods of calibration on models for which we do not yet have analytic solutions.

In our opinion, it is the final item in the above list that is of most importance for future investigation, since as we have found even for three parameter inference of $\{F, J, \gamma\}$ in our model, calibration is a difficult task without suitable data-sets. The collection of such data-sets (beyond that of the stock market) that can be used for calibration is therefore of great importance, especially given the need for policy makers to understand immediate challenges relating to the climate crisis and the transition to a more sustainable world [75]. As stated by Beinhocker in *The Origin of Wealth* [39], economists will get no sympathy from biologists and physicists who must go to great lengths to collect data to test their theories. Socio-economic modelling, and the models similar to that studied in this paper, can form an essential part of the work necessary to understand what policy makers need to do to change human collective behaviour in uncertain times.

Supporting information

S1 File.
(ZIP)

Acknowledgments

Author Contributions

Conceptualization: James Holehouse, Hector Pollitt.

Formal analysis: James Holehouse.

Investigation: James Holehouse.

Methodology: James Holehouse.

Resources: James Holehouse.

Visualization: James Holehouse.

Writing – original draft: James Holehouse.

Writing – review & editing: James Holehouse, Hector Pollitt.

References

1. Brock WA, Durlauf SN. Discrete choice with social interactions. The Review of Economic Studies. 2001; 68(2):235–260. https://doi.org/10.1111/1467-937X.00168

2. Borghesi C, Bouchaud JP. Of songs and men: a model for multiple choice with herding. Quality & quantity. 2007; 41(4):557–568. https://doi.org/10.1007/s11135-007-9074-6

3. Bouchaud JP. Crises and collective socio-economic phenomena: simple models and challenges. Journal of Statistical Physics. 2013; 151(3):567–606. https://doi.org/10.1007/s10955-012-0687-3

4. Hosseiny A, Absalan M, Sherafati M, Gallegati M. Hysteresis of economic networks in an XY model. Physica A: Statistical Mechanics and its Applications. 2019; 513:644–652. https://doi.org/10.1016/j.physa.2018.08.064

5. Weisbuch G, Kirman A, Herreiner D. Market organisation and trading relationships. The economic journal. 2000; 110(463):411–436. https://doi.org/10.1111/1468-0297.00531

6. Kirman A. Complex economics: individual and collective rationality. Routledge; 2010.

7. Moran J, Fosset A, Kirman A, Benzaquen M. From Ants to Fishing Vessels: A Simple Model for Herding and Exploitation of Finite Resources. Journal of Economic Dynamics and Control. 2021; p. 104169. https://doi.org/10.1016/j.jedc.2021.104169

8. Mézard M, Parisi G, Virasoro MA. Spin glass theory and beyond: An Introduction to the Replica Method and Its Applications. vol. 9. World Scientific Publishing Company; 1987.

9. Moran PAP. Random processes in genetics. In: Mathematical proceedings of the cambridge philosophical society. vol. 54. Cambridge University Press; 1958. p. 60–71.

10. Kirman A. Ants, rationality, and recruitment. The Quarterly Journal of Economics. 1993; 108(1):137–156. https://doi.org/10.2307/2118498

11. Moran J, Fosset A, Benzaquen M, Bouchaud JP. Schrödinger's ants: a continuous description of Kirman's recruitment model. Journal of Physics: Complexity. 2020; 1(3):035002.

12. Farmer R, Bouchaud JP. Self-Fulfilling Prophecies, Quasi Non-Ergodicity & Wealth Inequality. National Bureau of Economic Research; 2020.

13. Roberts K, Alberts B, Johnson A, Walter P, Hunt T. Molecular biology of the cell. New York: Garland Science. 2002.

14. Schnoerr D, Sanguinetti G, Grima R. Approximation and inference methods for stochastic biochemical kinetics—a tutorial review. Journal of Physics A: Mathematical and Theoretical. 2017; 50(9):093001. https://doi.org/10.1088/1751-8121/aa54d9

15. Milo R, Shen-Orr S, Itzkovitz S, Kashtan N, Chklovskii D, Alon U. Network motifs: simple building blocks of complex networks. Science. 2002; 298(5594):824–827. https://doi.org/10.1126/science.298.5594.824 PMID: 12399590

16. Peccoud J, Ycart B. Markovian modeling of gene-product synthesis. Theoretical population biology. 1995; 48(2):222–234. https://doi.org/10.1006/tpbi.1995.1027

17. Iyer-Biswas S, Hayot F, Jayaprakash C. Stochasticity of gene products from transcriptional pulsing. Physical Review E. 2009; 79(3):031911. https://doi.org/10.1103/PhysRevE.79.031911 PMID: 19391975

18. Braichenko S, Holehouse J, Grima R. Distinguishing between models of mammalian gene expression: telegraph-like models versus mechanistic models. bioRxiv. 2021. https://doi.org/10.1098/rsif.2021.0510 PMID: 34610262

19. Schwanhäusser B, Busse D, Li N, Dittmar G, Schuchhardt J, Wolf J, et al. Global quantification of mammalian gene expression control. Nature. 2011; 473(7347):337–342. https://doi.org/10.1038/nature10098 PMID: 21593866

20. Halpern KB, Tanami S, Landen S, Chapal M, Szlak L, Hutzler A, et al. Bursty gene expression in the intact mammalian liver. Molecular cell. 2015; 58(1):147–156. https://doi.org/10.1016/j.molcel.2015.01.027

21. Larsson AJ, Johnsson P, Hagemann-Jensen M, Hartmanis L, Faridani OR, Reinius B, et al. Genomic encoding of transcriptional burst kinetics. Nature. 2019; 565(7738):251–254. https://doi.org/10.1038/s41586-018-0836-1 PMID: 30602787

22. Suter DM, Molina N, Gatfield D, Schneider K, Schibler U, Naef F. Mammalian genes are transcribed with widely different bursting kinetics. science. 2011; 332(6028):472–474. https://doi.org/10.1126/science.1198817 PMID: 21415320

23. Herbach U, Bonnaffoux A, Espinasse T, Gandrillon O. Inferring gene regulatory networks from single-cell data: a mechanistic approach. BMC systems biology. 2017; 11(1):1–15. https://doi.org/10.1186/s12918-017-0487-0 PMID: 29157246

24. Brock WA, Durlauf SN. Interactions-based models. In: Handbook of econometrics. vol. 5. Elsevier; 2001. p. 3297–3380.

25. Sornette D. Physics and financial economics (1776–2014): puzzles, Ising and agent-based models. Reports on progress in physics. 2014; 77(6):062001. https://doi.org/10.1088/0034-4885/77/6/062001 PMID: 24875470

26. Amit D. The Ginzburg criterion-rationalized. Journal of Physics C: Solid State Physics. 1974; 7 (18):3369. https://doi.org/10.1088/0022-3719/7/18/020

27. Bouri E, Gupta R, Roubaud D. Herding behaviour in cryptocurrencies. Finance Research Letters. 2019; 29:216–221. https://doi.org/10.1016/j.frl.2018.07.008

28. Michael L, Otterbacher J. Write like I write: Herding in the language of online reviews. In: Eighth International AAAI Conference on Weblogs and Social Media; 2014.

29. Cornwall M. The determinants of religious behavior: A theoretical model and empirical test. Social forces. 1989; 68(2):572–592. https://doi.org/10.2307/2579261

30. Täuber UC. Critical dynamics: a field theory approach to equilibrium and non-equilibrium scaling behavior. Cambridge University Press; 2014.

31. Van Kampen NG. Stochastic processes in physics and chemistry. vol. 1. Elsevier; 1992.

32. Glauber RJ. Time-dependent statistics of the Ising model. Journal of mathematical physics. 1963; 4 (2):294–307. https://doi.org/10.1063/1.1703954

33. Nadal JP, Weisbuch G, Chenevez O, Kirman A. A formal approach to market organization: choice functions, mean field approximation and maximum entropy principle. Advances in Self-Organization and Evolutionary Economics. 1998; p. 149–159.

34. Mercure JF. FTT: Power: A global model of the power sector with induced technological change and natural resource depletion. Energy Policy. 2012; 48:799–811. https://doi.org/10.1016/j.enpol.2012.06.025

35. Mercure JF. Global electricity technology substitution model with induced technological change. Tyndall Centre on Global Climate Change Working Paper. 2011.

36. Anderson SP, De Palma A, Thisse JF. Discrete choice theory of product differentiation. MIT press; 1992.

37. Mercure JF, Pollitt H, Bassi AM, Viñuales JE, Edwards NR. Modelling complex systems of heterogeneous agents to better design sustainability transitions policy. Global environmental change. 2016; 37:102–115. https://doi.org/10.1016/j.gloenvcha.2016.02.003

38. McCullen NJ, Rucklidge AM, Bale CS, Foxon TJ, Gale WF. Multiparameter models of innovation diffusion on complex networks. SIAM Journal on Applied Dynamical Systems. 2013; 12(1):515–532. https://doi.org/10.1137/120885371

39. Beinhocker ED. The origin of wealth: Evolution, complexity, and the radical remaking of economics. Harvard Business Press; 2006.

40. King JE. Advanced introduction to post Keynesian economics. Edward Elgar Publishing; 2015.

41. Gillespie DT. Stochastic simulation of chemical kinetics. Annu Rev Phys Chem. 2007; 58:35–55. https://doi.org/10.1146/annurev.physchem.58.032806.104637 PMID: 17037977

42. Grauwin S, Bertin E, Lemoy R, Jensen P. Competition between collective and individual dynamics. Proceedings of the National Academy of Sciences. 2009; 106(49):20622–20626. https://doi.org/10.1073/pnas.0906263106 PMID: 19934061

43. Gardiner C. Stochastic methods. vol. 4. Springer Berlin; 2009.

44. Smith S, Shahrezaei V. General transient solution of the one-step master equation in one dimension. Physical Review E. 2015; 91(6):062119. https://doi.org/10.1103/PhysRevE.91.062119 PMID: 26172673

45. Pillai SU, Suel T, Cha S. The Perron-Frobenius theorem: some of its applications. IEEE Signal Processing Magazine. 2005; 22(2):62–75. https://doi.org/10.1109/MSP.2005.1406483

46. Weidlich W. The statistical description of polarization phenomena in society. British Journal of Mathematical and Statistical Psychology. 1971; 24(2):251–266. https://doi.org/10.1111/j.2044-8317.1971.tb00470.x

47. Bezanson J, Edelman A, Karpinski S, Shah VB. Julia: A fresh approach to numerical computing. SIAM review. 2017; 59(1):65–98. https://doi.org/10.1137/141000671

48. Munsky B, Khammash M. The finite state projection algorithm for the solution of the chemical master equation. The Journal of chemical physics. 2006; 124(4):044104. https://doi.org/10.1063/1.2145882 PMID: 16460146

49. Iserles A, MacNamara S. Applications of Magnus expansions and pseudospectra to Markov processes. European Journal of Applied Mathematics. 2019; 30(2):400–425. https://doi.org/10.1017/S0956792518000177

50. Tapias D, Paprotzki E, Sollich P. From entropic to energetic barriers in glassy dynamics: The Barrat–Mézard trap model on sparse networks. Journal of Statistical Mechanics: Theory and Experiment. 2020; 2020(9):093302. https://doi.org/10.1088/1742-5468/abaecf

51. Schnakenberg J. Network theory of microscopic and macroscopic behavior of master equation systems. Reviews of Modern physics. 1976; 48(4):571. https://doi.org/10.1103/RevModPhys.48.571

52. Ferrenberg AM, Xu J, Landau DP. Pushing the limits of Monte Carlo simulations for the three-dimensional Ising model. Physical Review E. 2018; 97(4):043301. https://doi.org/10.1103/PhysRevE.97.043301 PMID: 29758673

53. Morningstar A, Melko RG. Deep learning the ising model near criticality. arXiv preprint arXiv:170804622. 2017.

54. Cervera-Lierta A. Exact Ising model simulation on a quantum computer. Quantum. 2018; 2:114. https://doi.org/10.22331/q-2018-12-21-114

55. Horst U. Ergodicity and Non-Ergodicity in Economics. New Palgrave Dictionary of Economics, revised edition, L Blume and S Durlauf, eds. 2008.

56. Nakićenović N. Freeing energy from carbon. Daedalus. 1996; 125(3):95–112.

57. Farmer JD, Lafond F. How predictable is technological progress? Research Policy. 2016; 45(3):647–665. https://doi.org/10.1016/j.respol.2015.11.001

58. Foxon TJ. Technological and institutional 'lock-in'as a barrier to sustainable innovation. Imperial College Centre for Policy and Technology Working Paper. 2002.

59. Ashcroft P. Metastable States in a Model of Cancer Initiation. In: The Statistical Physics of Fixation and Equilibration in Individual-Based Models. Springer; 2016. p. 91–126.

60. Antal T, Scheuring I. Fixation of strategies for an evolutionary game in finite populations. Bulletin of mathematical biology. 2006; 68(8):1923–1944. https://doi.org/10.1007/s11538-006-9061-4 PMID: 17086490

61. Qin AK, Suganthan PN. Self-adaptive differential evolution algorithm for numerical optimization. In: 2005 IEEE congress on evolutionary computation. vol. 2. IEEE; 2005. p. 1785–1791.

62. Feldt R. BlackBoxOptim; 2021. https://github.com/robertfeldt/BlackBoxOptim.jl/blob/master/examples/benchmarking/latest_toplist.csv.

63. Horst R, Pardalos PM, Van Thoai N. Introduction to global optimization. Springer Science & Business Media; 2000.

64. The Economist. Forecasting the US elections; 2020. https://projects.economist.com/us-2020-forecast/president.

65. Toni T, Welch D, Strelkowa N, Ipsen A, Stumpf MP. Approximate Bayesian computation scheme for parameter inference and model selection in dynamical systems. Journal of the Royal Society Interface. 2009; 6(31):187–202. https://doi.org/10.1098/rsif.2008.0172 PMID: 19205079

66. Tankhilevich E, Ish-Horowicz J, Hameed T, Roesch E, Kleijn I, Stumpf MP, et al. GpABC: a Julia package for approximate Bayesian computation with Gaussian process emulation. Bioinformatics. 2020; 36 (10):3286–3287. https://doi.org/10.1093/bioinformatics/btaa078 PMID: 32022854

67. Öcal K, Grima R, Sanguinetti G. Parameter estimation for biochemical reaction networks using Wasserstein distances. Journal of Physics A: Mathematical and Theoretical. 2019; 53(3):034002.

68. Kirman AP. Whom or what does the representative individual represent? Journal of economic perspectives. 1992; 6(2):117–136. https://doi.org/10.1257/jep.6.2.117

69. Arthur WB. Foundations of complexity economics. Nature Reviews Physics. 2021; 3(2):136–145. https://doi.org/10.1038/s42254-020-00273-3 PMID: 33728407

70. Gallegati M, Kirman A. Beyond the representative agent. Edward Elgar Publishing; 1999.

71. Grauwin S, Goffette-Nagot F, Jensen P. Dynamic models of residential segregation: An analytical solution. Journal of Public Economics. 2012; 96(1-2):124–141. https://doi.org/10.1016/j.jpubeco.2011.08.011

72. Jia C, Grima R. Frequency domain analysis of fluctuations of mRNA and protein copy numbers within a cell lineage: theory and experimental validation. Physical Review X. 2021; 11(2):021032. https://doi.org/10.1103/PhysRevX.11.021032

73. Huang H. Hydrodynamic solution of the time-dependent Ising model. The Journal of Chemical Physics. 1979; 70(5):2390–2392. https://doi.org/10.1063/1.437747

74. Kumar M, Dasgupta C. Nonequilibrium phase transition in an Ising model without detailed balance. Physical Review E. 2020; 102(5):052111. https://doi.org/10.1103/PhysRevE.102.052111 PMID: 33327127

75. Masson-Delmotte, V, P Zhai, A Pirani, S L Connors, C Péan, S Berger, et al. IPCC, 2021: Summary for Policymakers. In: *Climate Change 2021: The Physical Science Basis. Contribution of Working Group I to the Sixth Assessment Report of the Intergovernmental Panel on Climate Change*. Cambridge University Press. In Press.